The Journal of Neuroscience, December 1, 1997, 17(23):9010–9025

Short-Term Changes in the Ca^{2+}-Exocytosis Relationship during Repetitive Pulse Protocols in Bovine Adrenal Chromaffin Cells

Kathrin L. Engisch, Natalya I. Chernevskaya, and Martha C. Nowycky

Department of Neurobiology and Anatomy, Medical College of Pennsylvania–Hahnemann University, Allegheny University of the Health Sciences, Philadelphia, Pennsylvania 19129

Stimulus-secretion coupling was monitored with capacitance detection in bovine chromaffin cells recorded in perforated patch mode and stimulated with trains of depolarizing pulses. A subset of stimulus trains evoked a response with a Ca^{2+}-exocytosis relationship identical to that obtained for single depolarizing pulses (Engisch and Nowycky, 1996). Other trains evoked responses with enhanced or diminished Ca^{2+} efficacy relative to this input–output function. The probability of obtaining a particular Ca^{2+}-exocytosis relationship was correlated with the amount of Ca^{2+} entry per pulse, such that shorter pulses or smaller currents were associated with the greatest efficacy, and longer pulses and larger currents with the lowest efficacy.

Apparent enhancements in Ca^{2+} efficacy were not caused by residual Ca^{2+} summing between pulses, because decreasing the interval between pulses usually reduced efficacy in the same cell; conversely, increasing the interval between pulses did not prevent an enhanced Ca^{2+}-exocytosis relationship. Apparent decreases in Ca^{2+} efficacy were not caused by depletion of an available pool of release-ready vesicles, because an equivalent amount of total Ca^{2+} entry during a single long depolarizing pulse usually evoked a much larger secretory response in the same cell. Finally, there were no striking differences in global Ca^{2+} levels monitored with the fluorescent indicator Fura Red that could account for apparent changes in Ca^{2+} efficacy during repetitive stimulus protocols. It appears that in chromaffin cells, the Ca^{2+}-exocytosis relationship is subject to activity-dependent changes during a stimulus train and can be modulated up or down from a basal state accessed by single pulse stimulations.

Key words: stimulus-secretion coupling; synaptic plasticity; facilitation; depression; residual calcium; vesicle pools; catecholamines; large dense-cored vesicles; capacitance detection; Ca^{2+} measurements; amperometry

At fast synapses the postsynaptic response evoked by action potential stimulation is not constant but is subject to activity-dependent changes, becoming larger or smaller depending on the parameters of stimulation (for review, see Magleby, 1987). Although long-term changes in synaptic efficacy may be responsible for various forms of memory, short-term changes may contribute to temporal information processing and rapid changes in secretory output (Sejnowski, 1996; Fisher et al., 1997; Zador and Dobrunz, 1997). Until recently, the lack of sufficiently sensitive techniques limited detection of short-term changes in nonsynaptic secretory cells. This has changed with the development of the capacitance detection technique (Neher and Marty, 1982).

When neuroendocrine and endocrine cells or large nerve terminals are stimulated by trains of depolarizing pulses, exocytosis can be detected as abrupt "jumps" in membrane capacitance (C_m). The C_m jumps evoked by individual pulses usually are nonuniform: typically, C_m jumps increase initially and then decrease in amplitude (Lim et al., 1990; Thomas et al., 1990; Augustine and Neher, 1992; Ämmäläet al., 1993; von Rüden and Neher, 1993; Horrigan and Bookman, 1994; Seward et al., 1995; Hsu and Jackson, 1996; Huang and Neher, 1996; Seward and Nowycky, 1996; Giovannucci and Stuenkel, 1997). By analogy with fast synapses, it has been suggested that C_m jump amplitudes increase because of Ca^{2+} accumulation during the beginning of a train (residual Ca^{2+} hypothesis) (Katz and Miledi, 1968). Ca^{2+} accumulation may directly affect the exocytotic trigger (Heinemann et al., 1993), contribute to recruitment of additional pools with different Ca^{2+} sensitivities (Horrigan and Bookman, 1994; Gillis et al., 1996; Giovannucci and Stuenkel, 1997), or fulfill "threshold" requirements for Ca^{2+} (Ämmälä et al., 1993; Seward et al., 1995; Seward and Nowycky, 1996; Giovannucci and Stuenkel, 1997). At fast synapses, diminished postsynaptic responses are commonly attributed to depletion of finite pools of release-ready vesicles, although postsynaptic receptor desensitization and Ca^{2+} current inactivation complicate interpretation. With capacitance detection, postsynaptic sensitivity is not an issue, and Ca^{2+} can be maintained at constant levels using photorelease of caged Ca^{2+}. A decline in the rate of capacitance increase during sustained elevation of intracellular Ca^{2+} has been interpreted as evidence for rapid depletion of release-ready vesicle pools (Neher and Zucker 1993; Thomas et al., 1993; Heidelberger et al., 1994; Heinemann et al., 1994).

In whole-cell mode, secretory responses are complicated by rundown and the presence of exogenous chelators (Augustine and Neher, 1992; Burgoyne, 1995; Seward and Nowycky, 1996), limitations that can be minimized with perforated-patch recordings

Received May 13, 1997; revised Sept. 16, 1997; accepted Sept. 18, 1997.

This work was supported by National Institutes of Health Grant NS27781 (M.C.N.), a grant from the Muscular Dystrophy Association (M.C.N.), and National Institutes of Health Training Grant 5T32HD07467 (N.I.C.). K.L.E. is an Edward Jekkal Muscular Dystrophy Fellow. We thank Dr. Alla Fomina for helpful discussions, Drs. Stanley Misler (Washington University) and Kirk Kawagoe (Axon Instruments) for advice on amperometry measurements, and Axon Instruments for the loan of a Digidata 2000 Image Lightning board and Axon Imaging Workbench software.

K.L.E. and N.I.C. contributed equally to this work.

Correspondence should be addressed to Martha C. Nowycky, Department of Neurobiology and Anatomy, Medical College of Pennsylvania–Hahnemann University, Allegheny University of the Health Sciences, 3200 Henry Avenue, Philadelphia, PA 19129.

(Horn and Marty, 1988). When intact bovine chromaffin cells are stimulated by single depolarizing pulses, exocytosis is a simple function of total Ca^{2+} entry regardless of current amplitude, number or type of Ca^{2+} channels, or pulse duration (Engisch and Nowycky, 1996). Here we examine the Ca^{2+}-exocytosis relationship during repetitive stimulation. Depending on the amount of Ca^{2+} entry per pulse and interpulse interval, the Ca^{2+}-exocytosis relationship was sometimes the same as that observed for single pulses, but was often enhanced or depressed relative to this relationship. Enhanced efficacy is unlikely to be caused by simple Ca^{2+} accumulation, because shorter interpulse intervals actually prevented enhancement. Depression is not caused by depletion of vesicle pools, because a single pulse could evoke a greater amount of exocytosis in the same cell. Thus, the Ca^{2+}-exocytosis relationship in adrenal chromaffin cells is subject to short-term changes induced by patterned activity.

MATERIALS AND METHODS

Chromaffin cell culture. Adult bovine adrenal chromaffin cells were prepared by collagenase digestion as described in Vitale et al., (1991) and cultured on collagen-coated glass coverslips as described previously (Engisch and Nowycky, 1996). Cells were used between day 3 and day 7 after plating; culture media were partially replaced on day 3 and day 6.

Electrophysiological recording solutions. The standard bath solution for recordings contained (in mM): (A) 130 NaCl, 2 KCl, 10 glucose, 10 Na-HEPES, 1 $MgCl_2$, 5 *N*-methyl-D-glucamine, and 5 $CaCl_2$, pH 7.2, with HCl; or (B) 130 NaCl, 2 KCl, 10 glucose, 10 Na-HEPES, 1 $MgCl_2$, 5 $CaCl_2$, pH 7.2, with NaOH. The perforated-patch solution contained (in mM): (A) 135 Cs-glutamate, 10 HEPES, 9.5 NaCl, 0.5 BAPTA, pH 7.2, with CsOH; or (B) 120 Cs-glutamate, 20 HEPES, 8 NaCl, 1 $MgCl_2$, 0.5 EGTA, pH 7.2, with CsOH.

Amphotericin B was included in the pipette solution according to one of the two following procedures: (A) A stock solution of amphotericin B (125 mg/ml in DMSO) was prepared every ~2 hr by ultrasonication and kept protected from light at room temperature. The stock was added to the internal solution (final concentration of amphotericin B, 0.5 mg/ml), and the solution was homogenized on a Pro-250 homogenizer for 5–10 sec immediately before use; (B) a stock solution of amphotericin B (150 mg/ml) was kept frozen in the dark at −20°C for up to 2 weeks. Internal solution was added to the frozen aliquot (final concentration of amphotericin B, 0.6 mg/ml) and sonicated for 10–20 sec. Pipettes were dipped briefly in amphotericin B-free internal solution and backfilled with amphotericin-containing solution.

Approximately equal numbers of cells were recorded in the pair of external/internal solutions labeled "A" and "B" (>50 each). Initially, each group was analyzed separately. Because no systematic differences were found, the data sets were pooled. In the figure legends, cell names beginning with "Chr" are from recordings in solution pair "B," and all others are from recordings in solution pair "A." All recordings were performed at room temperature (20–28°C), and cells were perfused continuously at a rate of 1–2 ml/min. CsOH was obtained from ICN Biochemicals (Aurora, OH), amphotericin B and glutamic acid from Calbiochem (La Jolla, CA), Na_4-BAPTA from Molecular Probes (Eugene, OR), and DMSO from Aldrich (Milwaukee, WI). All other chemicals were from Sigma (St. Louis, MO).

Capacitance detection. Capacitance measurements were performed using a List EPC-7 patch-clamp amplifier and a computer-based phase-tracking algorithm (Joshi and Fernandez, 1988; Fidler and Fernandez, 1989), as described previously (Seward et al., 1995). Data acquisition was initiated when the access conductance after patching became >70 nS (A) or >100 nS (B); access conductance usually stabilized at 100 nS (A) or 150 nS (B). The orthogonal phase angles for measuring capacitance and conductance were recalculated at the beginning of each capacitance trace, i.e., ~15–20 sec, by switching in a 500 kΩ resistor in series with ground. Ten sine waves were averaged, giving a time resolution of either 14 or 18 msec per capacitance point (486 or 386 IBM-PC compatible computer, respectively).

Stimulus protocols. Cells were held at −90 mV and depolarized to +20 mV for various durations as noted. The interpulse interval is the time between the end of one depolarization and the beginning of the next. To achieve a given interpulse interval experimentally, the time required for recording baseline current and allowing for channel closure after each pulse (i.e., the total duration of the current trace; see Figs. 1, 6) was subtracted from the desired interpulse interval, and the result was divided by the sampling rate per capacitance point. The quotient was used to set the number of capacitance points acquired between two depolarizing pulses; round-off can cause maximal errors of 6 or 8 msec for the 486- versus 386-based computer, respectively. A stimulus protocol was applied every ~90–180 sec.

Data analysis. Ca^{2+} entry, in picocoulombs, was calculated from integration of Ca^{2+} currents using limits that excluded the major portion of the Na^+ current. Before integration, currents were leak-subtracted with an average of four hyperpolarizing pulses. Capacitance changes were calibrated by a manual displacement of 100 fF in the capacitance compensation circuitry of the patch clamp. The amplitude of C_m jumps was determined from the difference between the average of 10 capacitance points before and after the depolarizing pulse (~140–180 msec). Horrigan and Bookman (1994) reported a slow capacitative transient evoked by depolarizing pulses unrelated to exocytosis in rat chromaffin cells. This transient is much faster in bovine chromaffin cells recorded without tetrodotoxin (τ = 16 msec) (Chow et al., 1996) and has a much smaller amplitude. As a further check for possible contamination, we analyzed many of the C_m responses to 5 msec duration pulses by comparing the last 3 points before depolarization to the last 3 points before the next depolarization. There was no significant difference from a 10-point average.

Derivation of the standard transfer function. The standard input–output Ca^{2+} entry-exocytosis relationship was derived as follows: C_m responses evoked by single pulses were fit by the function $\Delta C_m = g * (\Sigma Ca^{2+})^n$, varying g, a proportionality constant and n, the power, until χ^2 reached a minimum value, in 27 individual cells (Engisch and Nowycky, 1996). "ΔC_m" is in femtofarads, and "ΣCa^{2+}" is the integral of the Ca^{2+} current originally described in 10^7 ions, but in this report it is converted to picocoulombs. Curves generated by the 27 functions were averaged together in Origin (Microcal, Northampton, MA) to obtain a single curve that was in turn fit, giving $\Delta C_m = 0.147 * (\Sigma Ca^{2+})^{1.5}$ (standard transfer function). The plot of the standard transfer function is called the standard curve.

Classification of Ca^{2+}-exocytosis relationships. Capacitance responses were classified as those that followed the standard curve or were enhanced or depressed relative to the standard curve in two ways. (1) All of the plots of individual trains were overlaid on the standard curve and graded on the basis of visual inspection as following the curve, lying above it, or falling below. This was generally straightforward, with the exception of some 5 msec duration pulse trains with small amounts of exocytosis. The bar graphs in Figures 1–3 are generated from this method. (2) For the summary plot in Figure 4 and Table 1, the total amount of exocytosis and of Ca^{2+} entry for each train were compared with values generated by the function, $\Delta C_m = 0.147 * (\Sigma Ca^{2+})^{1.5}$. For trains with small amounts of total Ca^{2+} entry, trains were rated as following the standard relationship if they were within 20 fF of the predicted value. For trains with larger amounts of Ca^{2+} influx, ratios <0.8 were classified as depressed, whereas ratios >1.6 were classified as enhanced. Both methods gave similar final percentages.

Amperometry. Amperometric electrodes were manufactured according to Kawagoe et al. (1993). Briefly, a single 8 μm carbon fiber was inserted into a glass capillary and pulled on a two-stage microelectrode puller (Narishige, Tokyo, Japan). The fiber extending from the pulled end of the glass was cut with iridectomy scissors, and the tip was dipped in freshly prepared liquid epoxy. The epoxy was dried overnight at room temperature and then cured at 150°C for 2–24 hr. Electrodes were used within 1–3 d of manufacture, and the carbon fiber tip was cut with a scalpel blade immediately before recording. Carbon fiber electrodes were backfilled with a 1 M KCl solution, and held at +700 mV using a modified PC-501 amplifier (Warner Instruments, New Haven, CT); oxidative currents attributable to catecholamine release were measured in voltage clamp. After a seal was obtained and during perforation, a carbon fiber microelectrode was manipulated onto the top of a chromaffin cell until they touched. Amperometric events evoked by depolarization were acquired at 1 kHz in Axobasic on a second computer that was under control of the capacitance acquisition software. Catecholamine release was quantified by integrating the area under the amperometric trace during and for 200 msec after each depolarizing stimulus, regardless of the interpulse interval, and is expressed in picocoulombs. For display, amperometric traces were imported into Origin (vers. 3.5; Microcal, Northampton, MA) and digitally filtered with a Fourier algorithm. Am-

perometric spikes were identified by a peak fitting subroutine ("Pick Peaks") in Origin. In Figures 10 and 11, the final cumulative amperometric value was normalized to the total cumulative C_m change with no adjustments for the initial baseline or response to the first pulse. Cells recorded with amperometric electrodes are excluded from the data sets in Figures 1–9 and Table 1.

Measurement of average intracellular [Ca^{2+}]. Changes in average intracellular [Ca^{2+}] levels were monitored with the calcium-sensitive fluorescent indicator Fura Red (Molecular Probes). Cells were loaded by incubation in 5 μM Fura Red AM, 0.02% Pluronic F-127 in culture medium for 35–45 min at 37°C. Coverslips were rinsed with culture medium and returned to the incubator for up to 60 min before experiments.

Fura Red was excited at two wavelengths, 440 nm (Ca^{2+} insensitive) and 490 nm (Ca^{2+} sensitive). Light from a conventional Hg arc lamp was passed through one of two interference filters in a motorized filter wheel (Oriel, Stratford, CT) and was reflected via a dichromic mirror (RKP 510 nm) onto the cell. Emitted light passed through a barrier filter (580 nm). Measurements at the Ca^{2+}-insensitive wavelength were made only before and after stimulus protocols. At the end of some recordings, a solution with 10 μM ionomycin (Calbiochem) and 10 mM Ca^{2+} was perfused into the bath to obtain a fluorescence signal at saturating Ca^{2+} levels.

Light was collected by a Gen III camera, and images were processed via a Digidata 2000 Image Lightning board (Axon Instruments, Foster City, CA) installed on a second computer. Images were collected at one-half video frame rate so that an image was obtained every 66 msec or ~4 capacitance points. Filter switching, shutter opening, and video acquisition were controlled by the capacitance detection software.

Acquired images were processed using Axon Imaging Workbench (Axon Instruments). The total fluorescence of the cell was determined from the average intensity of pixels over the cell, and the digitized data were imported into Origin for further analysis. Changes in Ca^{2+} concentration were calculated as a fractional fluorescence change in F_{440}/F_{490}. In a series of control experiments we found that there was a slight increase in fluorescence measured at 440 nm excitation when Ca^{2+} concentration increased from zero (solution buffered with 10 mM EGTA) to 10 mM Ca^{2+} in the presence of ionomycin. Because of this error, we calculated that for a saturating signal fractional fluorescence would be underestimated by 10–15%, at most; because the maximal changes evoked by depolarization were much smaller, the error should be even less. Cells preloaded with Fura Red are excluded from the data sets in Figures 1–9 and Table 1.

RESULTS

Pulsatile Ca^{2+} entry can evoke secretion with the same efficacy as single pulses

We have shown previously that in chromaffin cells recorded with perforated-patch methods, the relationship between Ca^{2+} entry and exocytosis evoked by single pulses can be described by a simple transfer function of the form $\Delta C_m = g * (\Sigma Ca^{2+})^n$, where ΔC_m is the change in cell surface capacitance in femtofarads, g is a proportionality constant, and ΣCa^{2+} is the integral of the Ca^{2+} current that is raised to the nth power (Engisch and Nowycky, 1996). There is no reason a priori to expect that exocytosis during the intermittent Ca^{2+} entry of a train should be evoked with the same Ca^{2+} efficacy as during a single long pulse. For equivalent amounts of Ca^{2+} entry, the two stimulus paradigms differ in at least two ways: (1) the Ca^{2+} concentration beneath the membrane should be lower during a train, because Ca^{2+} domains around open Ca^{2+} channels collapse between depolarizations, and Ca^{2+} is removed by diffusion and uptake mechanisms; and (2) the total elapsed time is much longer during a train, allowing time-dependent processes to take place.

Remarkably, a significant fraction of pulse trains evoked responses that exactly or closely followed a standard Ca^{2+}-exocytosis transfer curve obtained by averaging input–output functions for single pulses in 27 cells (see Materials and Methods). Examples of three such responses, each from a different cell,

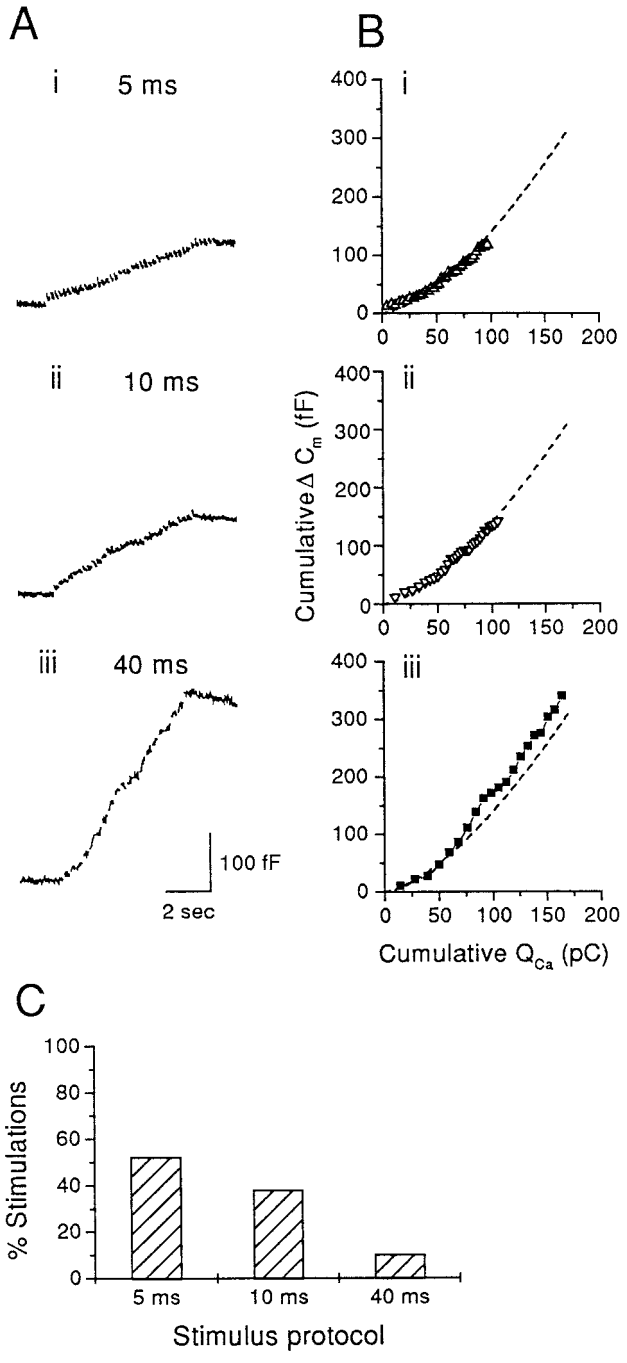

Figure 1. Exocytosis during trains of pulses can have the same relationship to Ca^{2+} entry as during single pulses. *A*, Capacitance traces from three different cells, stimulated with trains of (*A,i*) 5 msec duration, 40 pulses, (*A,ii*) 10 msec duration, 30 pulses, or (*A,iii*) 40 msec duration, 20 pulses. All stimulus trains had 200 msec intervals. Cells Chr175, N021702, L012504. *B*, For the same cells as in *A*, cumulative C_m increases replotted against cumulative Ca^{2+} current integrals. For these plots the Ca^{2+} current during each pulse was integrated and summed to previous Ca^{2+} entry. The *dashed curve* represents the standard transfer function obtained from a study of single pulse depolarizations in 27 cells [$\Delta C_m = 0.147 * (\Sigma Ca^{2+})^{1.5}$] (Engisch and Nowycky, 1996) (see Materials and Methods) and is not a fit to the data. *C*, Percentage of cells that responded to a given stimulus protocol with the same Ca^{2+}-exocytosis relationship as obtained on average from single pulse depolarizations. Only a single repetition of a given protocol is included per cell, although two or three different protocols were used per cell where possible. The total number of analyzed trains is 5 msec pulse duration, $n = 78$; 10 msec pulse duration, $n = 42$; 40 msec pulse duration, $n = 93$.

are shown in Figure 1. Without analysis, the C_m responses appear to differ greatly, with more exocytosis evoked by protocols with longer pulse durations and larger Ca^{2+} loads (Fig. 1*A*). However, when the same data are plotted as a function of the cumulative sum of Ca^{2+} current integrals for each pulse (Fig. 1*B*), the Ca^{2+}-exocytosis relationships for all three protocols are nearly identical to that evoked by single pulses: the dashed curve represents the standard curve and is not a fit of the data. Thus, in different cells an identical Ca^{2+}-secretion relationship can be evoked by train protocols that differ in the number of pulses, total elapsed time, and amount of Ca^{2+} influx per pulse.

The percentage of responses that obeyed the standard transfer function depended on the stimulus protocol (Fig. 1*C*). At fixed 200 msec interpulse intervals, stimulation with trains of 5 and 10 msec duration pulses evoked responses that followed the standard curve in >50% and 35% of chromaffin cells, respectively. Trains of 40 msec pulses evoked an exocytotic response with this pattern of Ca^{2+} efficacy in <10% of cells. The remaining responses were classified as being enhanced or depressed relative to the standard curve (see below).

Characteristics of exocytosis with enhanced Ca^{2+} efficacy

Examples of responses with greater Ca^{2+} efficacy than predicted by the standard transfer function are shown in plots of cumulative C_m changes versus cumulative Ca^{2+} entry (Fig. 2*A*) (three different cells). The C_m responses initially follow the standard Ca^{2+}-exocytosis relationship (*dashed curve*), but after a variable delay deviate to the left. Within the resolution limits imposed by noise in the C_m recording, the switch to enhanced Ca^{2+} efficacy appeared to be relatively abrupt. For example, in Figure 2*A,ii* the shift occurs after eight to nine pulses, whereas in Figure 2*A,i* after a few pulses, and in Figure 2*A,iii*, after only one pulse. Once a state of enhanced efficacy was achieved, cumulative C_m increases proceeded as a fairly linear function of cumulative Ca^{2+} entry, without either the upward curvature characteristic of the standard curve (Fig. 1) or the downward curvature of depressed responses (below and Fig. 3).

The percentage of cells that gave enhanced responses to trains of 5, 10, and 40 msec duration pulses is summarized in Figure 2*C*. Stimulation with 5 msec duration pulse trains evoked responses with enhanced efficacy in 33% of cells; 10 msec duration pulse trains did so in 28% of cells, and 40 msec duration pulse trains in only 2% of cells tested. In all cells, the voltage-gated Ca^{2+} current showed typical inactivation during a train (Fig. 2*B*; comparison of first and last current), with no evidence for activation of additional "facilitation" channels as described for calf chromaffin cells (Artalejo et al., 1991, 1994).

Characteristics of exocytosis with diminished Ca^{2+} efficacy

Some exocytotic responses to pulse trains proceeded with diminished Ca^{2+} efficacy; that is, they were depressed relative to the standard curve. Figure 3*A* illustrates typical examples of such responses evoked by protocols of brief pulses (5, 10, and 20 msec duration pulses; three different cells). The plots of cumulative C_m increases versus cumulative Ca^{2+} entry are approximately linear, deviating from the standard curve (*dashed curve*) because they lack upward curvature. In these examples, Ca^{2+} entry continues to elicit exocytosis throughout the stimulus train.

Three examples of diminished efficacy evoked by protocols with longer pulses (40 msec duration pulses) are shown in Figure

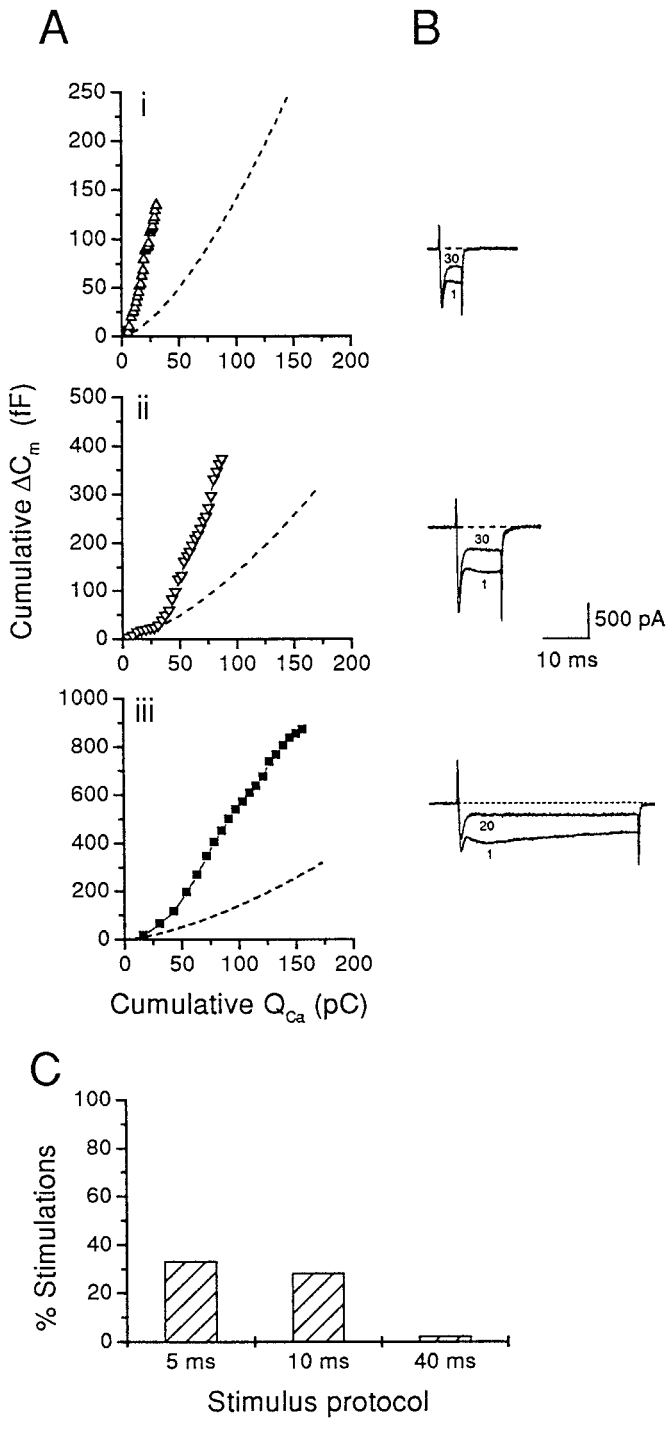

Figure 2. The Ca^{2+}-exocytosis relationship during pulse trains can be enhanced relative to the standard transfer function obtained from single pulse depolarizations. *A*, Cumulative C_m increases plotted against cumulative Ca^{2+} current integrals during a train from three different cells, stimulated with (*A,i*) 5 msec duration, 30 pulses, (*A,ii*) 10 msec duration, 30 pulses, (*A,iii*) 40 msec duration, 20 pulses. All pulses were given at 200 msec intervals. The *dashed curve* is a plot of the standard transfer function. Note the three different *y*-axis scales. Cells L012504, N122202, L012503. *B*, Superimposed first and last current trace for each stimulus train in *A*. The early rapidly decaying inward component is a Na^+ current. The Ca^{2+} current inactivates during all three stimulus trains, and there is no evidence for recruitment of a "facilitation" current (Artalejo et al., 1991). *C*, Percentage of cells that responded to a given stimulus protocol with a Ca^{2+} efficacy that was enhanced relative to the standard transfer function. Same data set as Figure 1*C* (see legend to Fig. 1).

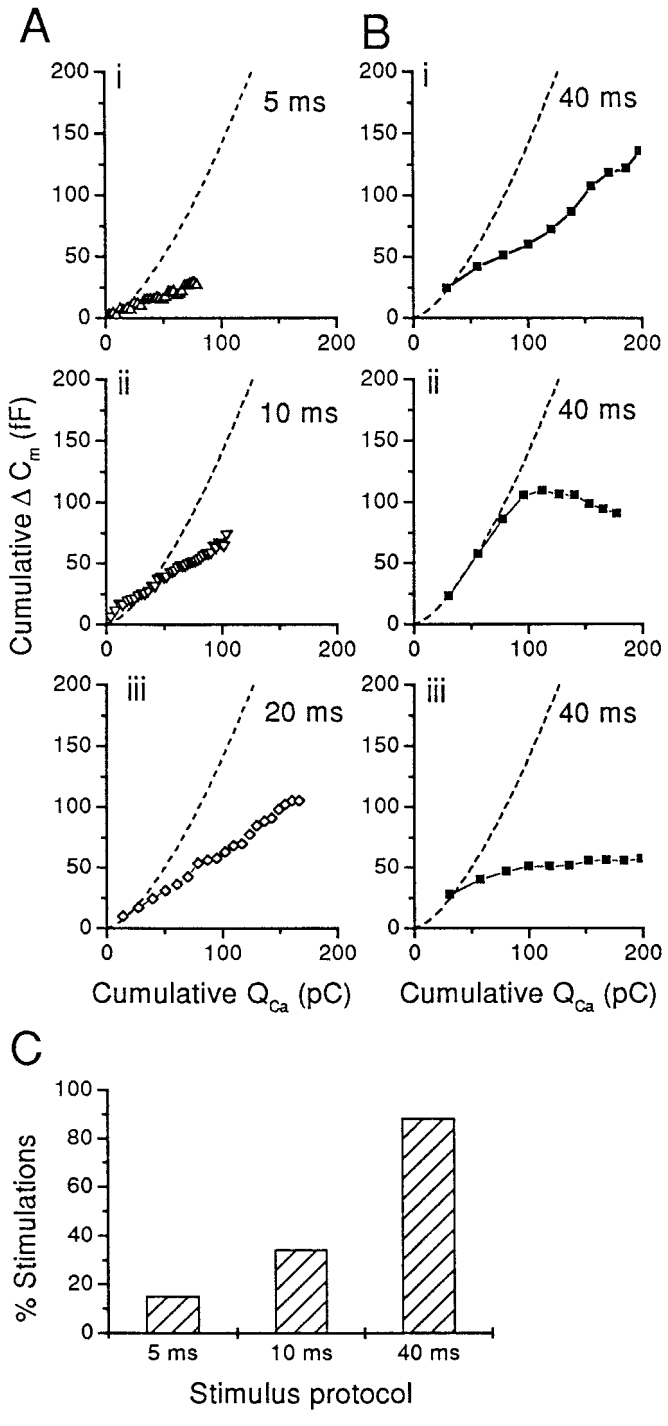

Figure 3. The Ca^{2+}-exocytosis relationship during pulse trains can be depressed relative to the standard transfer function obtained from single pulse depolarizations. *A*, Cumulative C_m increases from three different cells, stimulated with (*A,i*) 5 msec duration, 30 pulses, (*A,ii*) 10 msec duration, 30 pulses, (*A,iii*) 20 msec duration, 20 pulses. The *dashed curve* is a plot of the standard transfer function. Cells L031105, Chr110, Chr043. *B*, Cumulative C_m increases from three different cells stimulated with 40 msec duration, 10 pulses. Cells Chr171, Chr138, N012702. *C*, Percentage of cells that responded to a given stimulus protocol with a Ca^{2+} efficacy that was depressed relative to the standard transfer function. Same data set as Figures 1*C*, 2*C* (see legend to Fig. 1).

3*B*. In some cells (Fig. 3*B,i*), each pulse contributed additional C_m increases as during shorter pulse protocols (Fig. 3*A,i–iii*). In other cells, exocytosis ceased abruptly during the train, either after following the standard relationship for several pulses (Fig. 3*B,ii*) or for only a single pulse (Fig. 3*B,iii*).

Figure 3*C* summarizes the likelihood of obtaining a depressed response with each pulse protocol. Protocols of 40 msec duration pulses evoked responses with a diminished Ca^{2+}-exocytosis relationship in the majority of cells (~90%), whereas 10 msec duration pulse trains did so in 38% of cells. Trains of 5 msec duration pulses evoked depressed responses in a small but significant fraction of cells (~15%).

The three types of Ca^{2+} efficacies are correlated with the amount of Ca^{2+} entry per pulse

Under our culture and recording conditions, Ca^{2+} current amplitudes vary by as much as fivefold between cells. This allowed us to relate the likelihood of obtaining a particular Ca^{2+}-exocytosis relationship to the amount of Ca^{2+} influx during the first pulse of a train. A total of 219 capacitance responses were classified as having an enhanced, standard, or depressed Ca^{2+}-exocytosis relationship, with only one train of a given pulse duration included per cell. The data were binned by the integral of the first Ca^{2+} current, and the results are plotted as the percentage of responses within each bin.

Responses with enhanced Ca^{2+} efficacy are clearly correlated with the smallest amounts of Ca^{2+} entry (Fig. 4*A*). Exceptions do occur, however, as was illustrated for a 40 msec train in Figure 2*A,iii*. Responses that follow the standard curve are also associated with small amounts of Ca^{2+} entry (Fig. 4*B*), but they occur over a broader range, without the clear preference for the smallest Ca^{2+} current integrals. Depressed responses were evoked over the entire range of Ca^{2+} values, but the likelihood rose steadily with increasing Ca^{2+} entry during the first pulse (Fig. 4*C*). Trains of 40 msec duration pulses with average or larger than average Ca^{2+} currents always evoked depressed responses (integral $\geq 9 * 10^7$ ions or 28.8 pC; $n = 40$ cells).

Comparison of two stimulus protocols within individual cells: pulse duration

The histograms in Figure 4 indicate that the type of Ca^{2+}-exocytosis relationship is correlated with, but not a strict function of, Ca^{2+} entry per pulse. The data in Figures 1–4 were compiled by including only the first occurrence of a particular stimulus protocol per cell and therefore reflect the variability between cells. In the next four sections, we examine the capabilities of individual cells to respond to two different stimulus protocols.

We analyzed the exocytotic responses to a single pair of 5 and 40 msec duration pulse trains in 73 cells. In the majority of cells (~82%), Ca^{2+} efficacy was greater during the 5 msec train than during the 40 msec train. If the response to the 40 msec pulse train was depressed, that evoked by the 5 msec pulse train either followed the standard curve (Fig. 5*B*) or was enhanced (Fig. 5*C*). If the response to a 40 msec pulse train was not depressed, the 5 msec pulse train always evoked responses with enhanced Ca^{2+} efficacy (Fig. 5*D*). This is summarized in Figure 5*E*, where each bar represents the fraction of cells in which a pair of 5 and 40 msec pulse trains had the indicated Ca^{2+}-exocytosis relationships.

The only exceptions to this pattern were cells in which both trains evoked depressed responses (Fig. 5*A*; 15% of cells) and two cells (~3%) in which both trains evoked enhanced responses (not shown). Thus a few cells appear to be predisposed to enter a

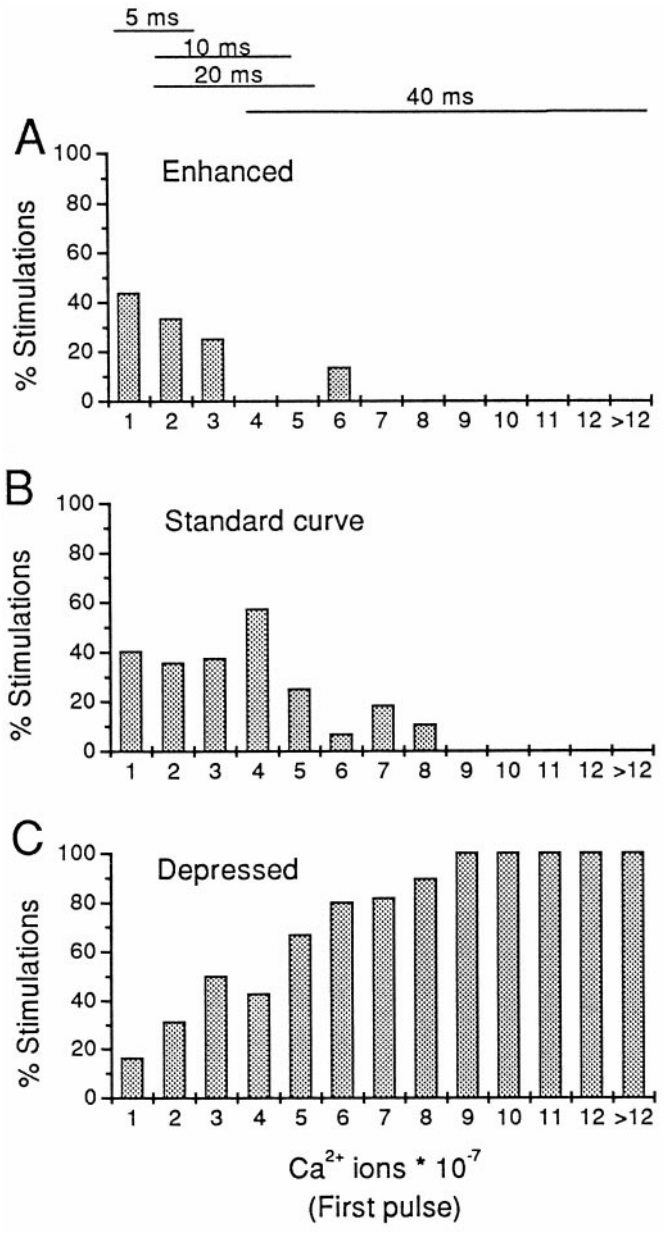

Figure 4. The Ca^{2+}-exocytosis relationship during a stimulus train is correlated with the amount of Ca^{2+} entry during the first pulse. Responses to 219 stimulus trains were classified and binned according to the integral of the Ca^{2+} current evoked by the first depolarizing pulse of a train in $1 * 10^7$ ion increments. The total experimental group consists of trains with pulse durations of 5 msec ($n = 78$), 10 msec ($n = 42$), 20 msec ($n = 6$), and 40 msec ($n = 93$); the range of Ca^{2+} entry during the first pulse of each stimulus paradigm is indicated by the *bars* above. Bins are labeled such that each contains values that range from its preceding neighbor to itself (i.e., the first bin contains stimuli with $0–1 * 10^7$ Ca^{2+} ions, whereas the second bin includes pulses with $1–2 * 10^7$ Ca^{2+} ions). The last bin contains all values $>12 * 10^7$ Ca^{2+} ions, with a maximal value of $20 * 10^7$ Ca^{2+} ions. Only the first train of any given protocol is included per cell, although for most cells, two or more different stimulus protocols are included. The response type was defined by the computer-based algorithm described in Materials and Methods as following the standard transfer function established by single pulse depolarizations, or being enhanced or depressed relative to this curve.

particular Ca^{2+}-exocytosis mode during repetitive stimulation. However, within a given cell, larger amounts of Ca^{2+} never evoked exocytosis with a higher efficacy ($n = 73$ cells).

Table 1. Comparison of responses to 5 and 40 msec duration pulse trains in individual cells

	5 msec trains		
	Depressed (%)	Standard curve (%)	Enhanced (%)
40 msec trains			
Depressed ($n = 38$)	29	63	8
St. C.–Depr. ($n = 25$)	0	32	68
St. Curve ($n = 8$)	0	0	100
Enhanced ($n = 2$)	0	0	100

Values represent the fraction of cells in each response category for 40 msec duration pulse trains (left) that had the indicated efficacy during a 5 msec duration pulse train. Same data set as Figure 5*E*. St. C.–Depr., Standard curve–depressed; St. Curve, standard curve.

Depressed responses to 40 msec trains were frequent ($n = 63/73$ cells), and we were able to subdivide this population further into two groups based on the timing of the shift to depression (e.g., compare Fig. 3*B,iii* with 3*B,ii*). Table 1 summarizes the results. Cells that became depressed quickly (1–3 pulses; "Depressed") account for the entire group of depressed responses to 5 msec pulse trains and otherwise usually followed the standard curve. Cells that followed the standard curve for more than three pulses before becoming depressed ("St. C.–Depr.") were more likely to respond to a 5 msec train with enhanced efficacy.

Thus, although the C_m response to a given amount of Ca^{2+} entry during a stimulus train cannot be predicted with certainty for any particular cell, changing the amount of Ca^{2+} entry per pulse results in an orderly, consistent shift between Ca^{2+}-exocytosis relationships within individual cells. At fixed interpulse intervals, this shift can be summarized by the following scheme:

$$\text{Depressed} \Rightarrow \text{St. Curve–Depressed} \Rightarrow \text{St. Curve} \Rightarrow \text{Enhanced}$$
$$\underline{\downarrow Ca^{2+}} \Rightarrow .$$

Comparison of two stimulus protocols within individual cells: Ca^{2+} concentration

We tested whether the shift between Ca^{2+}-exocytosis relationships depended in any way on the duration of depolarization by varying external Ca^{2+} concentrations (5 mM vs 0.3 or 0.5 mM). Figure 6 illustrates an experiment in which the response evoked by a 40 msec pulse train in 5 mM Ca^{2+} is depressed, and the response to a 5 msec pulse train follows the standard single-pulse relationship (*dashed curve*). In low Ca^{2+} (0.5 mM), the Ca^{2+} efficacy during a train of 40 msec pulses became identical to that evoked by a 5 msec train in 5 mM Ca^{2+}. In five such experiments, all cells had depressed responses during a 40 msec pulse train in 5 mM Ca^{2+}. In low Ca^{2+}, only one response remained depressed, two followed the standard curve, and two had enhanced efficacy. Thus diminished efficacy is induced by large amounts of Ca^{2+} entry rather than long depolarizations.

Comparison of single pulse and train protocols within individual cells

In this study, we define "depressed" or "enhanced" Ca^{2+} efficacy relative to a standard transfer function generated by averaging responses to single pulses in a separate cell population (see Materials and Methods). Ideally, the secretory responsiveness should be determined for each cell, but this was not feasible because of technical restrictions on the duration of patch-clamp

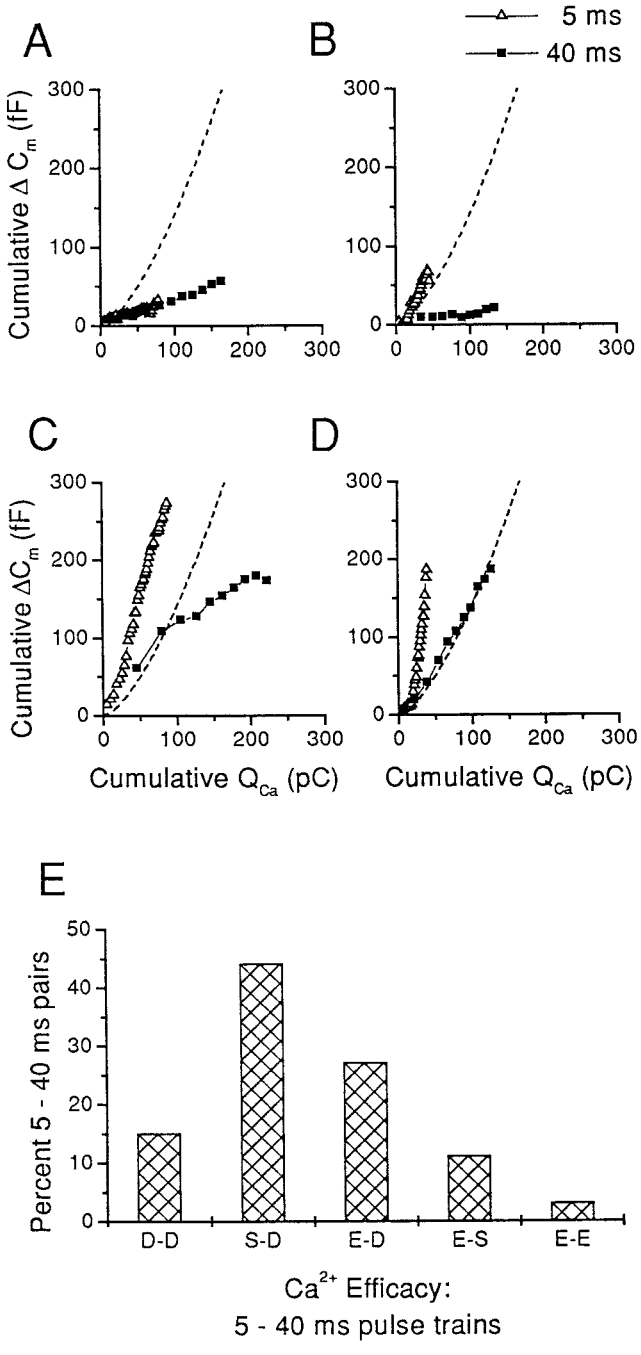

Figure 5. Trains of 5 msec pulses always evoke C_m responses with equal or greater Ca^{2+} efficacy than trains of 40 msec pulses in individual cells. *A–D*, Examples of capacitance responses to 5 and 40 msec pulse trains from four separate cells. In all panels, cumulative C_m increases are plotted against cumulative Ca^{2+} entry with the 5 msec (*open triangles*) and 40 msec duration pulse train (*closed squares*) superimposed. Cells were selected to illustrate pairs of responses that were (*A*) both depressed, (*B*) standard curve versus depressed, (*C*) enhanced efficacy versus depressed, (*D*) enhanced versus standard curve. Cells (*A*) Chr172, (*B*) N112704, (*C*) Chr061, (*D*) N122202. *E*, Percentage of cells stimulated with both 5 and 40 msec pulse trains that exhibit particular pairs of Ca^{2+} efficacy. The Ca^{2+}-exocytosis relationship for each 5 and 40 msec pulse train was classified as either depressed (*D*), enhanced (*E*), or one that obeys the standard transfer function (*S*) and expressed as a percentage of total cells stimulated with the two-pulse protocols ($n = 73$). In the majority of cells, 5 msec pulse trains evoked exocytosis with greater Ca^{2+} efficacy than 40 msec pulse trains (*S-D, E-D, E-S*), whereas in the remaining 18% the trains evoked responses with similar efficacies (*D-D, E-E*).

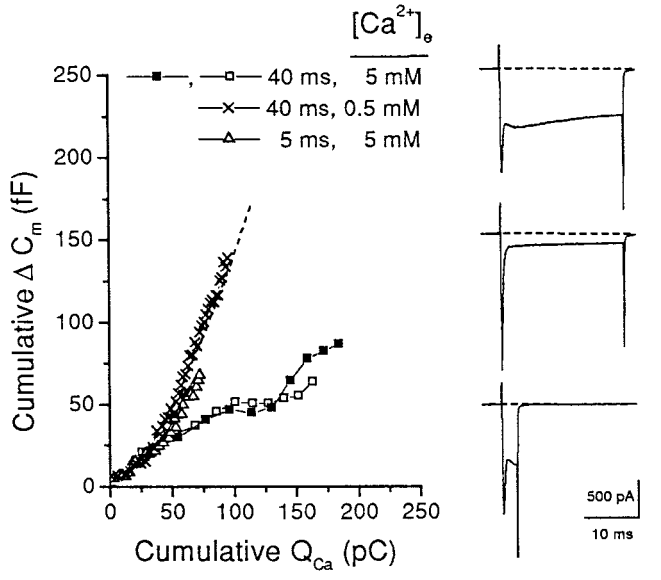

Figure 6. Long duration pulses in low extracellular $[Ca^{2+}]$ are equivalent to brief pulses in standard extracellular $[Ca^{2+}]$. Cumulative C_m responses from a single cell stimulated with two trains of 40 msec duration pulses and a train of 5 msec duration pulses in 5 mM extracellular $[Ca^{2+}]$, and a train of 40 msec duration pulses in 0.5 mM extracellular $[Ca^{2+}]$. The *dashed curve* represents the standard transfer function. The Ca^{2+} current evoked by the first pulse of each stimulus protocol is shown on the *right*. The current trace from only one of the two 40 msec duration pulse trains in 5 mM $[Ca^{2+}]$ is illustrated. Cell Chr0165.

recordings. However, the validity of using the standard transfer function can be checked by comparing the response to a single pulse and a stimulus train in a subset of cells.

We compared the total C_m increases evoked by a single 320 msec pulse and an equivalent amount of Ca^{2+} entry during a 40 msec train with 200 msec intervals. A total of 32 cells were stimulated with both protocols; as expected, most responses to the train had diminished efficacy. On average, the C_m increase during the 320 msec pulse was 1.8 times larger (Fig. 7*A,ii*). This is a minimum estimate of the relative efficacy of a 320 msec pulse and 40 msec pulse trains because (1) all responses to 40 msec pulse trains were included, although not all were depressed; and (2) this comparison ignores the final $\Delta C_m/\Sigma Ca^{2+}$ ratio during trains that was very low, because Ca^{2+} entry during later pulses was often completely unable to evoke C_m increases (e.g., Fig. 3*B,ii,iii*). We also observed (Fig. 7*A,i*) that a single 320 msec pulse could evoke a robust response even in cells most predisposed to depression during a repetitive pulse protocol, that is, the 15% that were depressed during both the 5 and 40 msec train (Fig. 5*A*, Table 1).

To examine a lower range of Ca^{2+} entry, we compared C_m responses evoked by a single 40 msec pulse and an equivalent amount of Ca^{2+} entry during a train of 5 msec duration pulses in 46 cells (Fig. 7*B,i,ii*). On average, a single 40 msec pulse was only half as effective at evoking exocytosis as a train of brief pulses. Again, this is a minimum estimate because <40% of cells had responses with enhanced efficacy during a train, yet all 5 msec pulse trains are included in this analysis. Thus, the changes in efficacy observed during repetitive pulse protocols are caused not by differences in the basal secretory responsiveness of cells but by activity-dependent mechanisms.

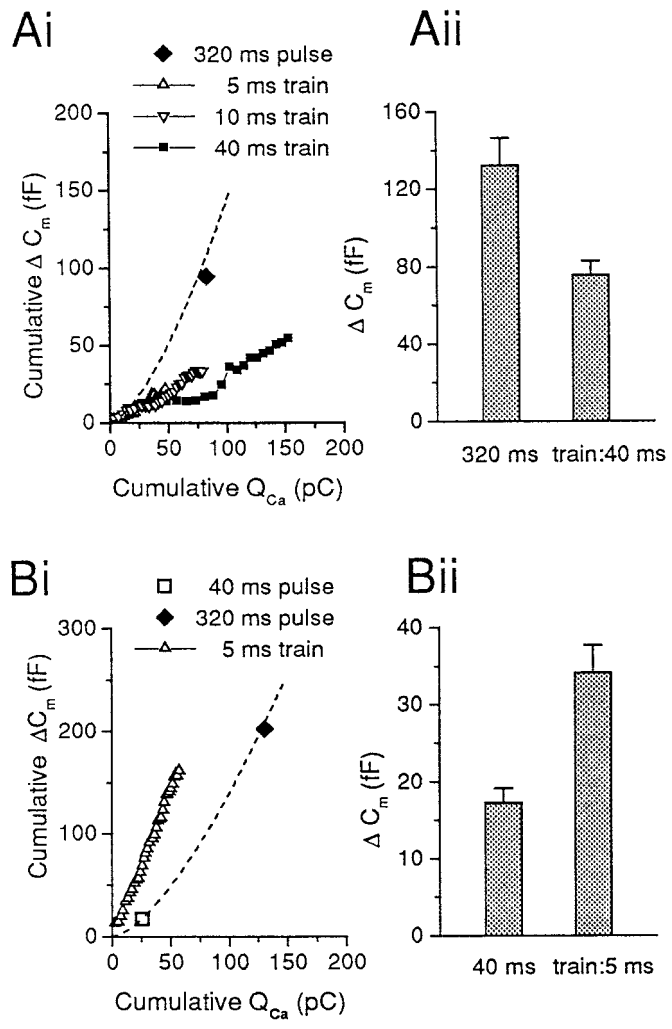

Figure 7. Stimulus trains consistently evoke changes in efficacy relative to single pulses. *A,i*, Responses of a single cell to four stimulus protocols as indicated. Plot of cumulative C_m increases against cumulative Ca^{2+} entry. In this example of a cell predisposed to depression, all three train protocols evoked depressed responses, but a single 320 msec pulse evoked a robust C_m jump that lies close to the standard curve (*dashed line*). Cell L082003. *A,ii*, Comparison of the response to a single 320 msec depolarization to the C_m increase evoked by an equivalent amount of Ca^{2+} entry during a 40 msec duration pulse train in 32 cells. Data represent mean ± SEM ($p < 0.001$; paired *t* test.) *B,i*, Responses of a single cell to three stimulus protocols as indicated. In this typical cell, the response to a 5 msec train is enhanced, and the response to a single 40 msec pulse (*open square*) and 320 msec pulse (*filled diamond*) lies close to the standard curve (*dashed line*). Cell L032704. *B,ii*, Comparison of the response to a single 40 msec pulse to the C_m increase evoked by an equivalent amount of Ca^{2+} entry during a 5 msec train in 46 cells. Data represent mean ± SEM ($p < 0.001$; paired *t* test).

Comparison of two stimulus protocols within individual cells: pulse interval

The previous sections describe the different exocytotic responses obtained when the amount of Ca^{2+} entry is altered at a constant interpulse interval (200 msec). To examine whether the exocytotic response of a cell is also influenced by the time span between bouts of Ca^{2+} entry, we tested various interpulse intervals.

Trains of 40 msec pulses at 200 msec intervals evoked depressed responses in most cells (Figs. 3*C*, 4). Prolonging the interpulse interval increased the Ca^{2+} efficacy without significant changes to total Ca^{2+} entry (Fig. 8). Three examples comparing a 200 and a 1000 msec interval stimulus train within individual cells are shown in Figure 8*A*. Cells with strong depression during the 200 msec train showed a partial relief of depression at 1000 msec intervals (Fig. 8*A,i*) or followed the standard curve (Fig. 8*A,ii*), whereas cells with less depression often gave large responses with enhanced Ca^{2+} efficacy (Fig. 8*A,iii*). A summary of 17 experiments is presented in Figure 8*B*, in which the total C_m increase evoked by the two protocols is compared. Despite the large variability of total ΔC_m during the 200 msec train, all data points cluster along a line with slope = 2. Thus within individual cells, there is a systematic shift of Ca^{2+} efficacy, remarkably similar to the shift that is observed as pulse duration is decreased at a constant interpulse interval (Fig. 5, Table 1). The shift was graded with the duration of the interpulse interval: at 400 msec intervals, there was no significant change, whereas at 800 msec responses were 1.35 times larger and at 1000 msec were two times larger (Fig. 8*C*).

We also tested the effect of shorter intervals during 40 msec duration pulse trains because this should approach the limit of a single prolonged pulse (0 msec interval) and possibly prevent the development of depression. Of all stimulus protocols tested, 40 msec pulses at 100 msec intervals gave the least consistent results. In 3 of 11 cells, depression was abolished at the shorter interval as predicted. However, in five cells the Ca^{2+}-exocytosis relationship was unchanged, one cell showed more depression, and two cells had rapid endocytosis. Thus although there is a slight tendency toward less depression at short intervals, the responses are too variable for further study.

The effect of shortening interpulse intervals during trains of 5 msec duration pulses depended on the response evoked by a train with 200 msec intervals. In five of six cells with enhanced Ca^{2+} efficacy during a 200 msec interval train, trains with shorter intervals evoked exocytosis with reduced efficacy (Fig. 9*B,i*). Figure 9*A* illustrates one such experiment. Two trains with 200 msec intervals evoked exocytosis with enhanced efficacy (Fig. 9*A,i,iii*), whereas the Ca^{2+}-exocytosis relationship during a 44 msec interval train followed the standard curve (Fig. 9*A,ii*). On the other hand, in six cells whose response followed the standard curve during 200 msec intervals, shortening the interval had little effect (Fig. 9*B,ii*). As suggested above, both results are expected if brief interpulse intervals approach the limiting condition of a single long pulse from which the standard transfer function is obtained and if enhanced efficacy is a departure from this basal responsiveness.

In Figure 9*A*, the higher frequency train (Fig. 9*A,ii*) induced slightly more total Ca^{2+} entry than either 200 msec interval train (Fig. 9A*i,iii*). This was a consistent finding in all cells tested: on average total Ca^{2+} entry was 1.12-fold greater during the higher frequency, 5 msec duration pulse trains (SEM = 0.03; $n = 12$; $p < 0.01$; paired *t* test). It appears that in addition to exocytosis, Ca^{2+} current inactivation is also subject to frequency-sensitive modulation in chromaffin cells.

Increasing the interpulse interval from 200 msec to 1000 msec had little effect on the Ca^{2+}-exocytosis relationship evoked by 5 msec pulse trains. The results are summarized in Figure 9*C* for seven cells. All values lie close to the dashed line that represents equivalency.

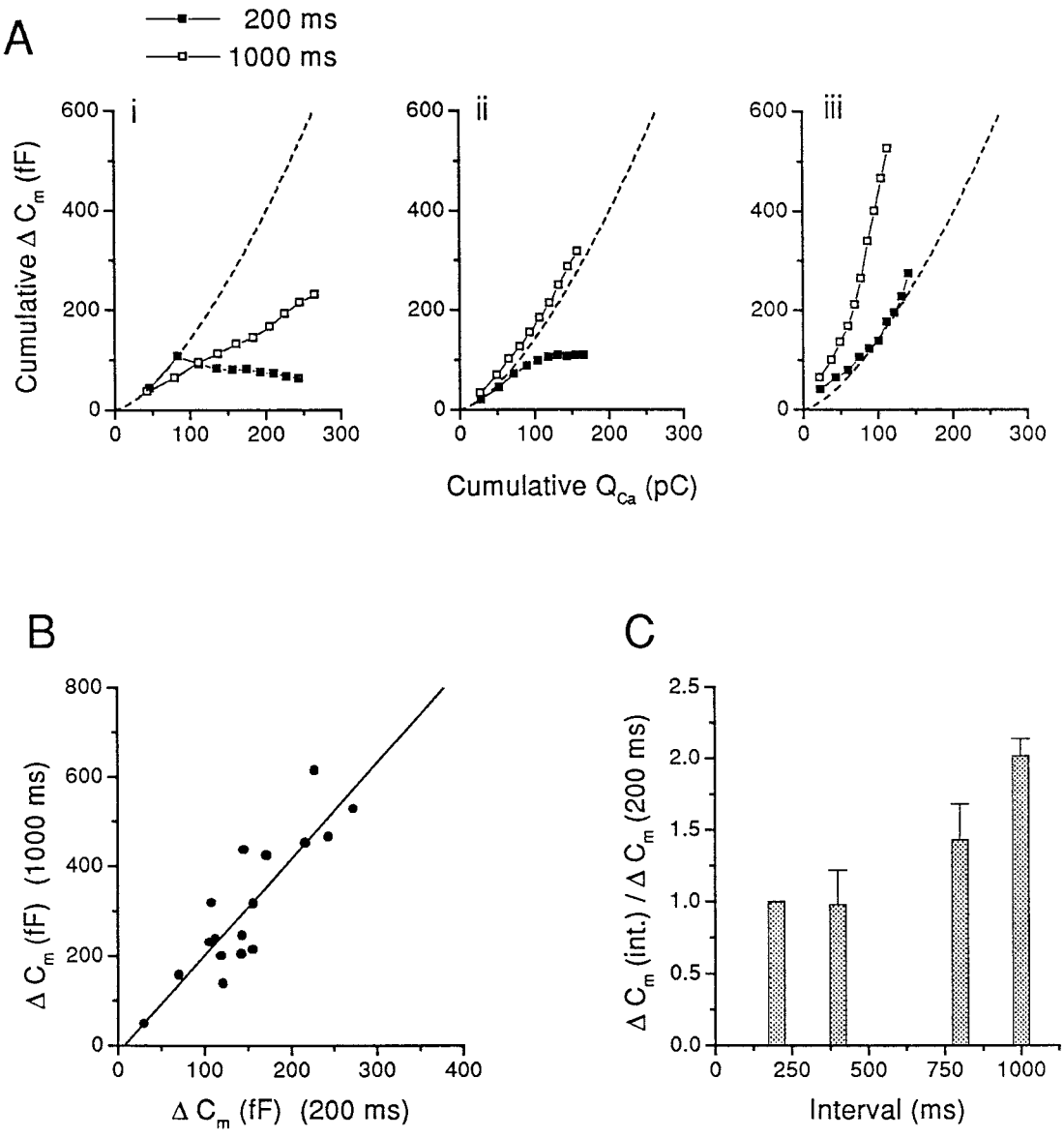

Figure 8. Longer interpulse intervals increase the Ca^{2+} efficacy of 40 msec duration pulse trains. *A*, Examples of capacitance changes in three cells stimulated with two 40 msec pulse protocols, at 200 and 1000 msec intervals. In all panels, cumulative C_m increases are plotted against cumulative Ca^{2+} entry with the two trains superimposed. The *dashed curve* represents the standard transfer function. Examples of (*A,i*) two depressed responses, (*A,ii*) a depressed response at 200 msec intervals and a response that follows the standard curve at 1000 msec intervals, and (*A,iii*) a response that follows the standard curve at 200 msec intervals and has enhanced efficacy at 1000 msec intervals. Cells Chr058, Chr059, and Chr200. *B*, Comparison of the total C_m responses evoked by a 200 msec versus 1000 msec interval stimulus protocol, 40 msec duration, 10 pulses, in individual cells. The *line* represents the best fit by linear regression and has slope = 2.15 ($r = 0.87$; $n = 17$). *C*, The total C_m increase for a given test interpulse interval was normalized to the total C_m increase elicited by a 40 msec duration, 200 msec interval stimulus in the same cell. Test protocols had intervals of 400 msec ($n = 5$), 800 msec ($n = 4$), or 1000 msec ($n = 17$). Data are presented as mean ± SD.

Amperometric recordings confirm that ΔC_m measurements reflect exocytosis of catecholamine-containing vesicles

The capacitance detection method reports only net changes of plasma membrane area. The apparent depression of exocytosis may be caused by simultaneous membrane removal by endocytosis. On the other hand, the apparent enhancement may actually be caused by the addition of some other type of membrane. For example, exocytosis of small synaptic vesicles versus large dense-cored vesicles is evoked by different Ca^{2+} levels (Verhage et al., 1991) and stimulus patterns (Bruns and Jahn, 1995). Finally, apparent enhancement may result from totally artifactual sources such as gating charge movement (Horrigan and Bookman, 1994). These issues can be resolved with amperometric techniques that specifically detect the release of catecholamines (Wightman et al., 1991).

Simultaneous capacitance and amperometric recordings of a typical strongly depressed response to a train of 40 msec duration pulses, 200 msec intervals are shown in Figure 10*A*. The amperometric events are few, and all occur during the early part of the train when the C_m trace shows a small increase. The cumulative integral of the amperometric signal initially rises in parallel with the C_m response but is flat during the rest of the train (Fig. 10*A, bottom*), indicating that catecholamine release and C_m increases

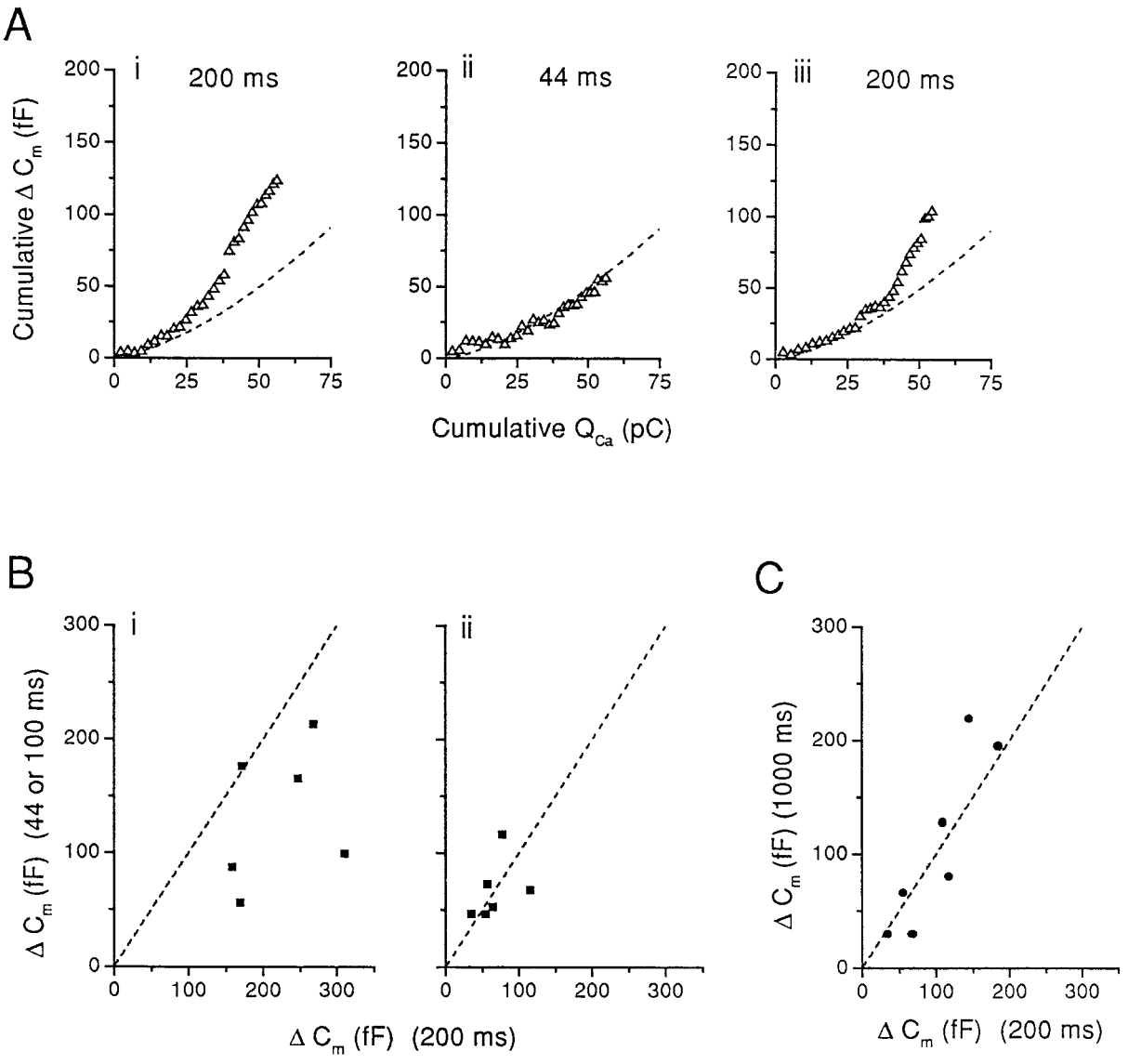

Figure 9. Shorter interpulse intervals can decrease Ca^{2+} efficacy of 5 msec duration pulse trains. *A*, Example of single cell stimulated with three trains. The stimulus protocol consisted of 5 msec duration, 30 pulses, at either 200 msec intervals (*A,i* and *A,iii*) or 44 msec interpulse intervals (*A,ii*). Stimulus trains in *A,i* and *A,iii* were applied just before and after the stimulus train in *A,ii*. Cumulative C_m increases are plotted against cumulative Ca^{2+} entry. The *dashed curve* is a plot of the standard transfer function. The Ca^{2+}-exocytosis relationship is enhanced at the longer interval but follows the standard curve during the shorter interval. Note that there was slightly more total Ca^{2+} entry in *A,ii*, typical for higher frequency protocols (see text). Cell N041002. *B*, Comparison of total C_m responses in 12 cells stimulated with two trains of 5 msec duration pulses, at 200 msec intervals and either 44 or 100 msec intervals. Cells were divided into those that had an enhanced response during the 200 msec train (*i*, total $\Delta C_m > 150$ fF) or those that followed the standard curve (*ii*, total $\Delta C_m < 150$ fF). The *dashed line* has a slope of 1 and represents equivalent responses during the two trains. *Points* below the line indicate that the higher frequency train evoked a smaller total C_m response. *C*, Comparison of total C_m responses in seven cells stimulated with two trains of 5 msec duration pulses, at 200 msec and 1000 msec intervals. The range of C_m values in this plot is smaller than in *B* because the lower frequency trains contained fewer total pulses and the total C_m responses were compared for an equivalent number of pulses in each train. Most points fall on or near a line with slope = 1 (*dashed line*), indicating equal amounts of C_m increase during the two stimulus protocols.

stop simultaneously. Amperometric events occurred only during the first few pulses in five of six cells with depressed C_m responses to 40 msec trains.

The cell shown in Figure 10*A* was also stimulated with a train of 40 msec duration pulses, but with 1000 msec intervals (Fig. 10*B*). As described above (Fig. 8), longer interpulse intervals typically relieve depression; here, the C_m response closely follows the standard curve (*bottom*). Amperometric events occurred throughout the entire duration of the train, mirroring the persistence of C_m jumps. Because of the relatively long interval between pulses, endocytotic processes are clearly visible as declines in the C_m trace. As a result, the difference between the pre- and post-train C_m level appears to be ~100 fF for both trains (Fig. 10*A,B, top*). In calculating ΔC_m for cumulative plots, we used only the first 200 msec after each pulse (see Materials and Methods). This calculation gives a total ΔC_m change of ~250 fF (Fig. 10*B, bottom*) and a ~2.5 times increase over the 200 msec interval train. Q_{amp} is similarly increased by approximately three times. These data confirm that C_m changes parallel catecholamine release and indicate that endocytotic processes are too slow to mask exocytosis during 200 msec interval protocols.

Figure 11 contains an example of a cell in which a 5 msec

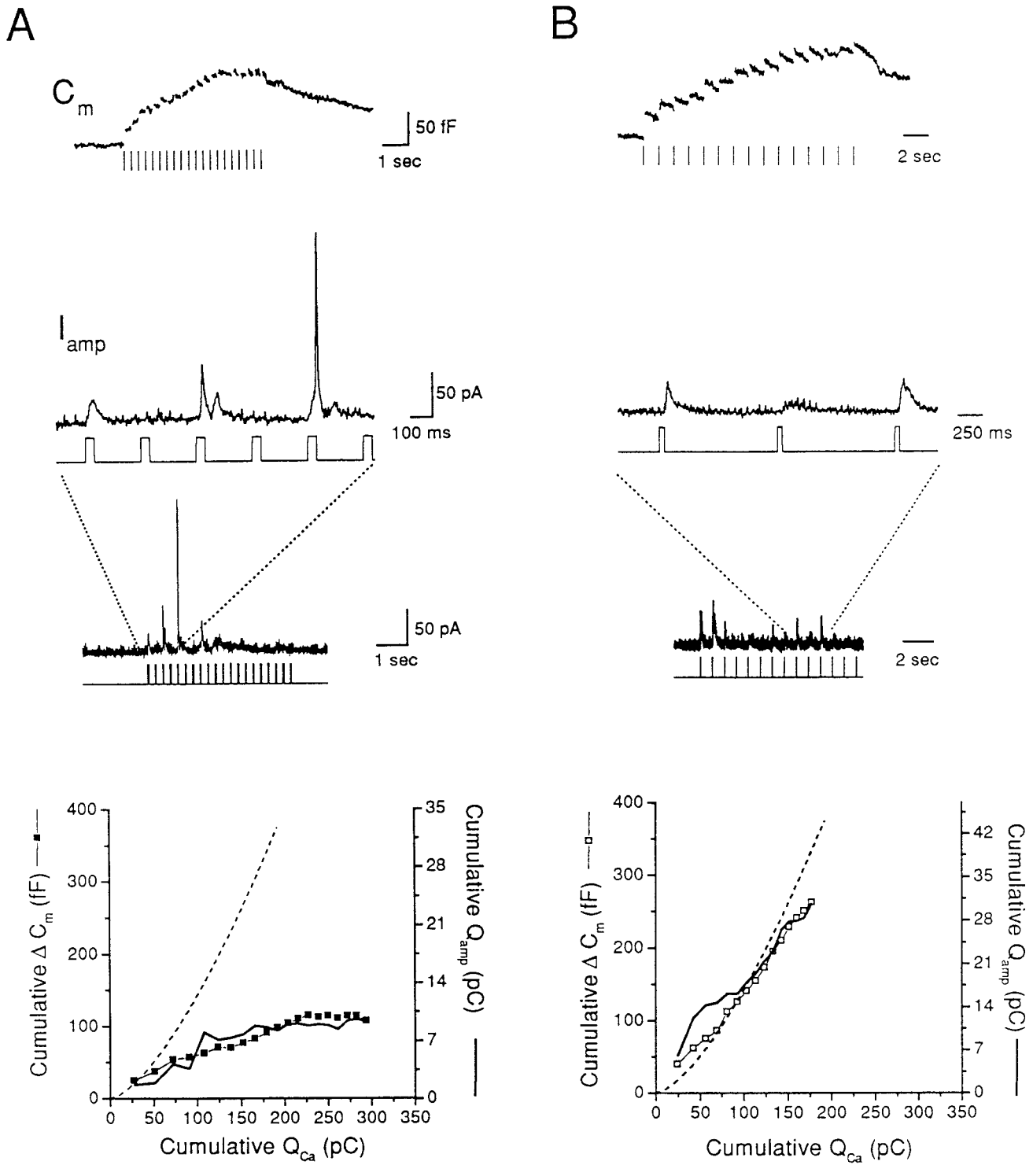

Figure 10. "Depressed" capacitance responses are not an artifact of simultaneous endocytosis. *A, Top trace* (C_m): Capacitance trace from a cell stimulated with 40 msec duration pulses at 200 msec intervals (20 pulses). Timing of depolarizations is indicated by *gaps* in the trace and by the *vertical bars* below. *Middle traces* (I_{amp}): Amperometric recording during the same stimulus shown on an expanded (*above*) and compressed (*below*) time scale. Timing of depolarizations is indicated below each trace. *Bottom*, *Left axis*: Plot of cumulative C_m increases against cumulative Ca^{2+} entry. The *dashed curve* is a plot of the standard transfer function. The Ca^{2+}-exocytosis relationship of this cell is strongly depressed. *Right axis*: The amperometric signal during the stimulus train was integrated and is expressed in picocoulombs. For comparison to the capacitance response, the maximum amperometric response was aligned with the maximum C_m increase and plotted against cumulative Ca^{2+} entry (*solid line*). *B*, The same cell was stimulated with 40 msec duration pulses at 1000 msec intervals (15 pulses). Calculation of ΔC_m was performed by using only the first 200 msec after each depolarization. Calculation of Q_{amp} was performed by integrating the current during and for 200 msec after each depolarization. All traces, plots, and vertical scales as in *A*. Cell L080104.

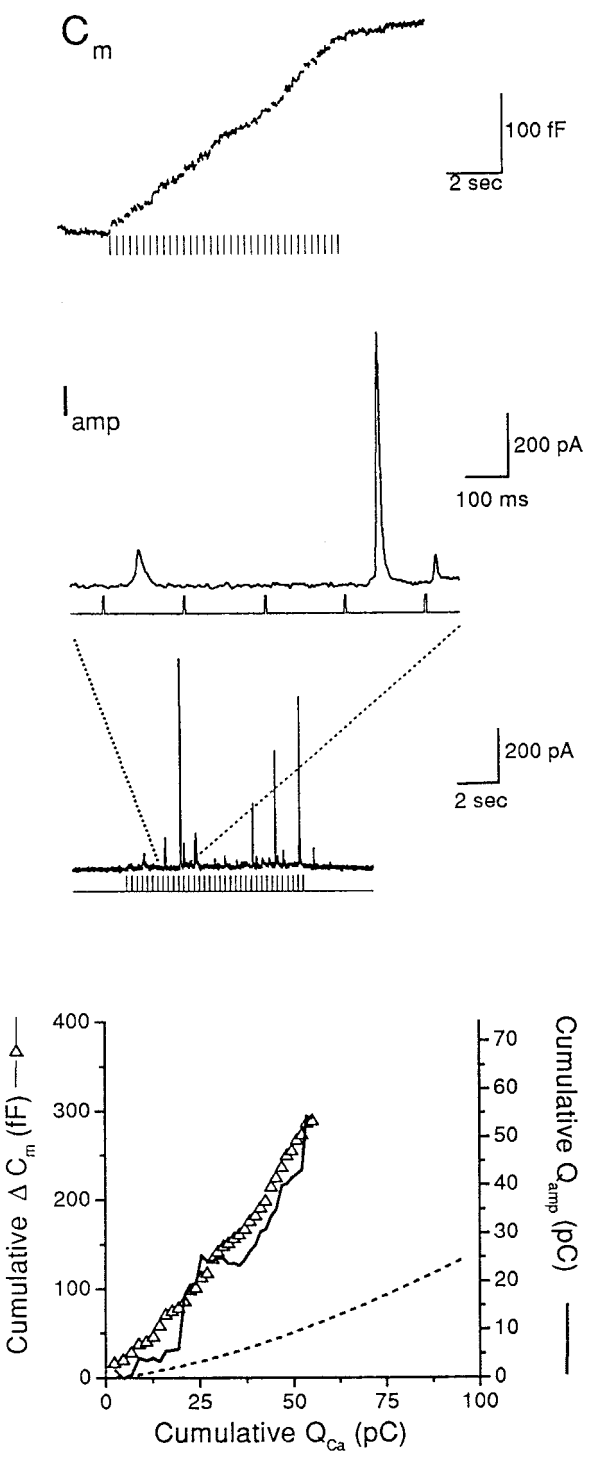

Figure 11. Amperometric recordings confirm that C_m increases with enhanced Ca^{2+} efficacy reflect exocytosis of catecholamine-containing vesicles. *Top trace* (C_m): Capacitance trace from a cell stimulated with 5 msec duration pulses, 200 msec intervals (35 pulses). Timing of depolarizations is indicated by *gaps* in the two traces and by the *vertical bars* below. *Middle traces* (I_{amp}): Amperometric recording during the same stimulus shown on an expanded (above) and compressed (below) time scale. Timing of depolarizations is indicated by the *vertical steps*. *Bottom plot*: *Left axis:* Plot of cumulative C_m increases against cumulative Ca^{2+} entry. The *dashed curve* is a plot of the standard transfer function. *Right axis*: The amperometric signal during the stimulus train was integrated and is expressed in picocoulombs. For comparison with the capacitance response, the maximum amperometric response was aligned with the maximum C_m increase and plotted against cumulative Ca^{2+} entry (*solid line*). Cell L061703.

duration pulse train evoked a capacitance response that was strongly enhanced relative to the standard curve. The capacitance trace (C_m, *top*) has small, step-like increases throughout the train. In the amperometric recording, large upward spikes are uniformly scattered throughout the duration of the stimulus (I_{amp}). In cells that had an enhanced response to a 5 msec duration pulse train, there were more spikes than in cells with responses that followed the standard transfer function (0.25 events/pulse, $n = 4$, vs 0.057 events/pulse, $n = 4$, respectively). This confirms that the enhancement of Ca^{2+} efficacy is attributable to the addition of membrane from catecholamine-containing vesicles. Amperometric recordings also rule out the possibility that the apparent C_m changes are caused by an artifact such as an ion channel gating charge, which might be particularly prominent in a long train of brief pulses (Horrigan and Bookman, 1994; Engisch and Nowycky, 1996).

Changes in Ca^{2+}-exocytosis relationships are not caused by differences in global $[Ca^{2+}]_i$

An apparent increase in the efficacy with which Ca^{2+} entry evokes exocytosis may actually be caused by Ca^{2+} contribution by intracellular stores. On the other hand, apparent diminished efficacy may result from the recruitment of rapid Ca^{2+} clearing mechanisms after large amounts of Ca^{2+} influx (Rorsman et al., 1992, Peng and Zucker, 1993; Hehl et al., 1996), or they may be caused by inhibitory effects of high $[Ca^{2+}]_i$. To determine this, we monitored fluorescence in cells preloaded with the Ca^{2+}-sensitive dye Fura Red AM.

Typical fluorescence changes evoked by four stimulus protocols in a single cell are illustrated in Figure 12. A single 320 msec pulse caused a rapid rise in global $[Ca^{2+}]_i$ that peaked ~40 msec after the pulse (Fig. 12*A,i*). A train of 40 msec duration pulses, 200 msec intervals, evoked a $[Ca^{2+}]_i$ rise to the same peak level within the first three to four pulses (Fig. 12*A,ii*) that was maintained despite further doubling of Ca^{2+} entry between the fourth and tenth pulse (data not shown). During a train of 5 msec pulses, 200 msec intervals, $[Ca^{2+}]_i$ also rose to a plateau level, but this level was reached later and the final value was lower than during the 40 msec pulse train (Fig. 12*A,iii*). Finally, during a train of 40 msec pulses given at 1000 msec intervals, the maximal fluorescence signal was nearly identical to the plateau level of the 200 msec interval train; however, the signal decayed between each pulse (Fig. 12*A,iv*).

The fluorescence changes shown in Figure 12 are representative for chromaffin cells recorded in perforated-patch mode. The plateau level reached during a 40 msec duration, 200 msec interval train was linearly related to the peak change induced by a single 320 msec duration pulse (Fig. 12*B*). In contrast, the plateau levels reached during 5 msec duration pulse trains were consistently lower than those of 40 msec duration pulse trains (Fig. 12*C*). Peak changes and plateau values probably represent physiological processes rather than dye saturation. The plateau values of 40 msec duration trains were considerably lower than the maximal ratio after ionomycin application ($R_{max}/R_p = 1.77 \pm 0.16$; $n = 6$).

The fluorescence responses described here are representative of most recordings (14/18 cells). There were two exceptions to these patterns (data not shown). In two cells, the fluorescence response to the first 40 msec duration pulse train was approximately two times as large as that to all subsequent trains, although it also settled at a plateau by the third or fourth pulse. In two other cells, the plateau value was unusually small during various train protocols. Several seconds after each train, the fluorescence

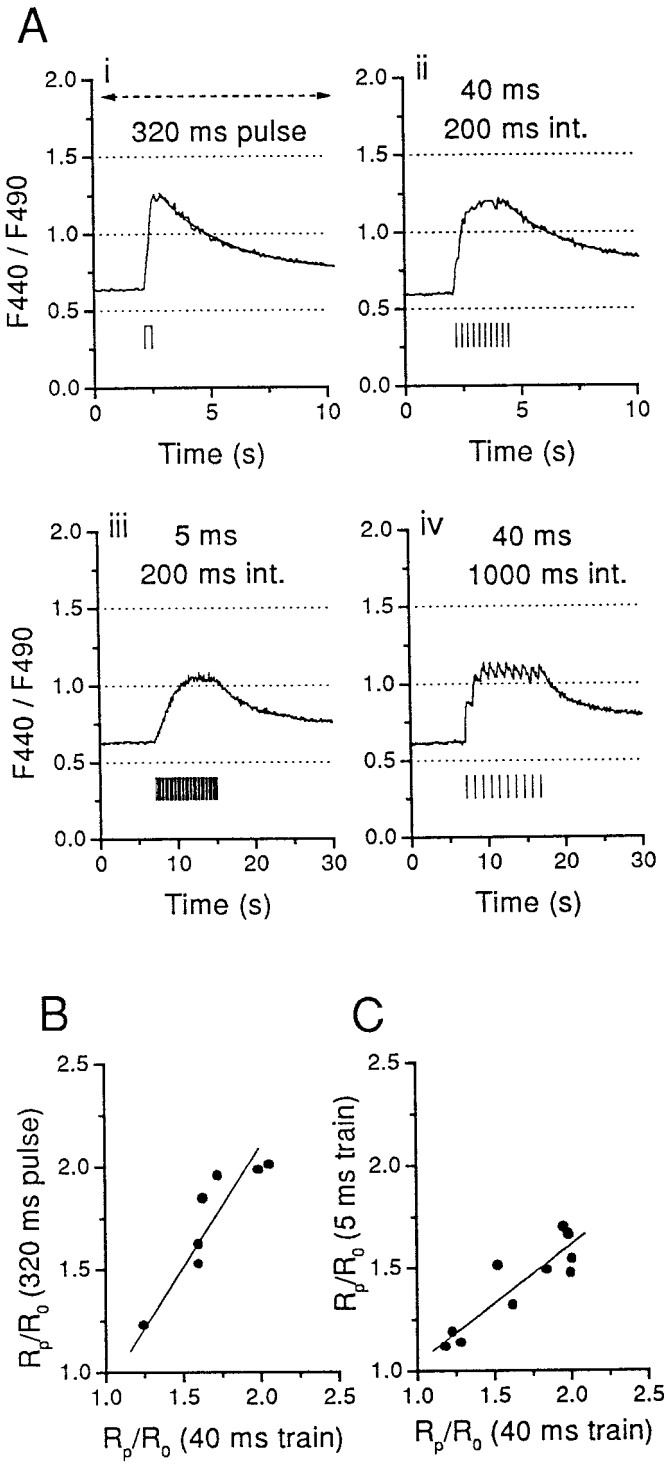

Figure 12. Average $[Ca^{2+}]_i$ is rapidly elevated to plateau levels during trains of depolarizing pulses in bovine chromaffin cells recorded in perforated patch mode. *A*,*i*–*iv*, Four fluorescence ratios from a single cell loaded with Fura Red AM evoked by (*i*) a single 320 msec depolarization; (*ii*) train of 40 msec duration, 200 msec interval, 10 pulses; (*iii*) train of 5 msec duration, 200 msec interval, 40 pulses; (*iv*) train of 40 msec duration, 1000 msec interval, 10 pulses. All stimuli are indicated by *bars* below the trace. Traces in *i* and *ii* are shown on expanded time scale, and each are fit with a single exponential with $\tau = 2.8$ and 3.5 sec, respectively. The *dashed line* in *i* represents the fluorescence ratio when ionomycin (10 μM) in external solution containing 10 mM $CaCl_2$ was applied at the end of the experiment to saturate the Ca^{2+}-sensitive dye. Cell Chr240. *B*, Plot of changes in fluorescence evoked by 40 msec duration pulse train versus signal rose abruptly to a much higher level and then fell, resembling an active "$[Ca^{2+}]$ spike." This was never accompanied by a C_m increase.

In summary, bovine chromaffin cells recorded in perforated patch mode appear to be much more effective at clamping $[Ca^{2+}]_i$ during stimulus trains than cells recorded in whole-cell mode (Augustine and Neher, 1992; Seward and Nowycky, 1996). There is no obvious correlation between $[Ca^{2+}]_i$ changes and the exocytotic Ca^{2+} efficacy evoked by particular stimulus protocols. Unexpectedly, loading cells with Fura Red and performing Ca^{2+} measurements caused several disturbances in the C_m responsiveness (data not shown). These include (1) poor reproducibility for two identical protocols in individual cells; (2) disruption of the systematic relationship of Ca^{2+} efficacies between pairs of different stimuli within cells (e.g., 5 msec duration pulse trains occasionally evoked responses with lower efficacy than 40 msec pulse trains); (3) unusual patterns that were not observed in control conditions (e.g., 5 msec duration pulse trains that had enhanced efficacy during the early pulses and complete depression during later pulses); and (4) occasional unusually large C_m jumps in response to the first pulse of 40 msec trains (84 ± 20 fF evoked by 7.5 ± 0.3 pC; $n = 54$ responses in 18 cells) (compare with Fig. 7*B*,*ii*). Both the intracellular Ca^{2+} handling properties and exocytotic responses in the presence of Ca^{2+} chelators require further investigation for chromaffin cells recorded in perforated-patch mode.

DISCUSSION

Summary

The key observation in this paper is that bovine chromaffin cells recorded in perforated-patch mode have a repertoire of Ca^{2+}-exocytosis relationships that are preferentially evoked by repetitive stimulus protocols. A simple standard transfer function adequately predicts the relationship between Ca^{2+} entry and amount of exocytosis when cells are stimulated with single depolarizing pulses (Engisch and Nowycky, 1996). Remarkably, the same transfer function applies to a subset of responses evoked by trains of depolarizing stimuli (Fig. 1). However, trains also evoke exocytosis with enhanced or diminished Ca^{2+} efficacy relative to this function. Exocytotic responses with enhanced Ca^{2+} efficacy are evoked preferentially by protocols associated with small amounts of Ca^{2+} entry per pulse, whereas diminished or "depressed" responses are induced by protocols that evoke larger amounts of Ca^{2+} entry per pulse. Changes in Ca^{2+} efficacy during repetitive stimulation are not determined solely by the amount of Ca^{2+} entry per pulse, but by the balance between Ca^{2+} entry and the interpulse interval. Prolonging the interval of 40 msec duration pulse trains shifts the response pattern from depression to following the standard curve or enhanced efficacy, whereas shortening

←

changes in fluorescence during a single 320 msec duration pulse. The change is expressed as the ratio of maximum signal during stimulation (R_p) to the signal before stimulation (R_0). The *line* is a best fit with slope = 0.84 ($r = 0.9$; $n = 7$). The average total Ca^{2+} entry during a single 320 msec duration pulse was 95 pC, whereas during 40 msec pulse trains, a plateau signal was achieved on average in 3.4 pulses at a cumulative Ca^{2+} current integral of 77 pC ($n = 11$). *C*, Plot of changes in fluorescence ratio evoked by a 5 msec duration pulse train versus a 40 msec duration pulse train in the same cell. The *line* is a best fit with slope = 0.57 ($r = 0.9$; $n = 11$). During 5 msec duration pulse trains, a plateau signal was achieved on average in 16 pulses at a cumulative Ca^{2+} entry of 36.8 pC ($n = 11$).

the interval of 5 msec duration pulse trains can prevent the development of an enhanced response. Our working hypothesis is that the single pulse relationship represents the "basal" Ca^{2+}-exocytosis relationship, in the absence of Ca^{2+}- and time-dependent modulatory processes. Both enhancement and depression develop during trains lasting several seconds and fade during the 2–5 min between stimulus trains, qualifying them as "short-term changes" in Ca^{2+} efficacy.

Capacitance responses to trains can obey the single-pulse transfer function

The observation that pulse trains can evoke C_m responses with the same Ca^{2+}-exocytosis relationship as single pulses is unexpected. Pulsatile Ca^{2+} entry during a train will create very different submembrane $[Ca^{2+}]$ profiles than will a continuous long depolarization (Sala and Hernandez-Cruz, 1990; Nowycky and Pinter, 1993; Klingauf and Neher, 1997). As was emphasized in Engisch and Nowycky (1996), the standard transfer function does not relate exocytosis to submembrane $[Ca^{2+}]$, but simply serves as a predictor for the total exocytosis expected for a given amount of Ca^{2+} entry. If intermittent Ca^{2+} entry during the many short pulses of a train can evoke a Ca^{2+}-exocytosis relationship with the same upward curvature as a single long pulse, some components of the secretory machinery must be able to "remember" or "sum" Ca^{2+} entry across interpulse intervals. Another surprising feature is the fidelity with which the C_m responses to trains often adhered to a curve generated by averaging functions from 27 cells, which had a range of individual g and n values (Engisch and Nowycky, 1996, their Table 1). In effect, the many pulses in a train appear to average out the variability of single-pulse responses both within and between cells.

Enhanced Ca^{2+} efficacy

Various forms of facilitation during trains of action potentials or depolarizing pulses have been described at both fast synapses and in whole-cell recordings of neuronal terminals, neuroendocrine, and endocrine cells (see introductory remarks). Commonly, most forms of facilitation are postulated to result from (1) an accumulation of intracellular or submembrane Ca^{2+} [variants of the "residual Ca^{2+}" or "residual Ca^{2+}-bound receptor" hypothesis (Katz and Miledi, 1968; Yamada and Zucker, 1992; Zucker, 1996)], (2) the existence of additional vesicular pools that are recruited during a train (Horrigan and Bookman, 1994; Gillis et al., 1996), or (3) requirements for an initial Ca^{2+}-dependent priming step (Seward and Nowycky, 1996). Here, explanations (2) and (3) can be considered as specialized versions of the residual Ca^{2+} hypothesis, in that experimentally increasing the amount of Ca^{2+} entry will more quickly achieve the condition in which there is additional exocytosis. An alternative form of facilitation is produced by the recruitment of Ca^{2+} channels that are preferentially coupled to exocytosis (Artalejo et al., 1994).

Enhanced Ca^{2+} efficacy as described here differs qualitatively from all forms of the residual Ca^{2+} hypothesis because it is evoked under conditions of minimal Ca^{2+} entry. In most cells, shortening the interpulse intervals, a condition that should accentuate Ca^{2+} accumulation, actually abolished enhanced responses. This is predicted by our working hypothesis that enhanced efficacy is a Ca^{2+}- and activity-dependent shift from the basal responsiveness of a cell. Enhanced efficacy is not caused by recruitment of "facilitation" channels, because Ca^{2+} currents exhibited typical inactivation during a train (Fig. 2). Finally, simultaneous capacitance and amperometric recording provide evidence that enhanced efficacy, defined by changes in the C_m trace, accurately reflects changes in the secretion of catecholamine-containing vesicles.

Diminished Ca^{2+} efficacy

Most models of secretory depression invoke the rapid depletion of release-ready vesicles (see introductory remarks). In our recordings, depression was associated with protocols that caused more Ca^{2+} entry, and depletion might be expected because of increased exocytosis. However, the total amount of exocytosis during a depressed response was much less than could be evoked in the same cell with a single long pulse, although the train spanned a time period that might be used for increasing the readily releasable pool. Depressed C_m responses are not the result of endocytotic processes masking exocytotic events, because simultaneous amperometric recordings verify that spike frequency declined concurrently (Fig. 10). Because capacitance recordings of isolated cells do not have the complications of postsynaptic changes, we can conclude that in chromaffin cells depression is a modulation of excitation–secretion coupling mechanisms that is actively induced by repetitive stimulation, independently of the vesicles available for release by a single pulse.

Most chromaffin cells have a repertoire of Ca^{2+}-exocytosis relationships

A limitation of the present study is that enhanced and depressed Ca^{2+} efficacies are not defined by unique quantitative criteria, but only relative to the standard transfer function. Pulse trains of 40 msec were usually easily classified, as were 5 msec pulse trains with enhanced efficacy. The only problematic groups were responses evoked by 5 msec pulse trains that were either depressed or followed the standard curve, because of the small absolute C_m changes (usually a few tens of femtofarads, or several large dense-cored vesicles, assuming 2.0–2.5 fF/vesicle). Nevertheless, the distribution of response patterns is highly reproducible between cells and is a useful starting point for further study.

Under our culture conditions, most chromaffin cells appear to have a repertoire of Ca^{2+}-exocytosis efficacies, with only a few that are depressed or have enhanced efficacy in response to both a 5 and a 40 msec duration pulse train (Fig. 5). This latter group may have greater amounts of the factors responsible for activity-dependent changes during stimulus trains, because at least some cells had typical responses to single-pulse depolarizations. Within the majority of cells, there is an orderly progression of Ca^{2+}-secretion relationships from:

$$\text{Enhanced} \Rightarrow \text{Standard curve} \Rightarrow \text{Depressed},$$

as the amount of Ca^{2+} entry per pulse is increased at fixed interpulse intervals or as the interpulse interval is decreased for a given pulse duration. In summary, activity-dependent changes in the exocytotic responsiveness of bovine chromaffin cells appear to be determined by both the balance of Ca^{2+} entry per pulse and the interpulse interval.

Intracellular Ca^{2+} measurements

In whole-cell recordings of many cell types and nerve terminals, fluorescence measures of average intracellular Ca^{2+} are usually proportional to the amount of Ca^{2+} entry until they reach dye saturation, although the relationship is not necessarily linear (Thomas et al., 1990; Augustine and Neher, 1992; Ämmälä et al., 1993; Mollard et al., 1995; Seward and Nowycky, 1996). Excep-

tions do occur: neurohypophysial nerve terminals successfully clamp average $[Ca^{2+}]_i$ at ~500 nM regardless of Ca^{2+} load, unless the mitochondria are poisoned (Stuenkel, 1994). Bovine chromaffin cells in perforated-patch mode appear to regulate $[Ca^{2+}]_i$ much more strictly than cells recorded in whole-cell mode. During repetitive pulse trains, a plateau in fluorescence is achieved that appears to represent a set-point to which $[Ca^{2+}]_i$ is clamped. The similarity between the average $[Ca^{2+}]_i$ evoked by the various stimulus protocols rules out the possibility that shifts between the various Ca^{2+}-exocytosis relationships result from global elevation of $[Ca^{2+}]_i$ and instead suggests that they are caused by intermittent Ca^{2+} elevations near the plasma membrane that are dissipated before they can be detected with our techniques.

Possible mechanism of short-term changes in Ca^{2+} efficacy

Many second messenger systems, cytoskeletal elements, and other agents can modify stimulus-secretion coupling of large dense-cored vesicles (for review, see Burgoyne, 1991). Capacitance techniques have sufficient temporal resolution and sensitivity to detect modulation at a single cell level. Activation of protein kinase C enhances the amount of exocytosis in chromaffin cells (Vitale et al., 1995; Gillis et al., 1996) and lactotrophs (Fomina and Levitan, 1995), whereas cyclosporin A, an inhibitor of calcineurin, a Ca^{2+}-calmodulin-dependent type 2B phosphatase, depresses exocytosis in bovine chromaffin cells (Engisch and Nowycky, 1997). In pancreatic β-cells, exocytosis is potentiated by activation of protein kinase C and protein kinase A, or by inhibition of Ca^{2+}-calmodulin kinase II and type I and 2A phosphatase (Ämmälä et al., 1993, 1994). The repetitive stimulus protocols used here span several seconds, which provides sufficient time for Ca^{2+}-dependent activation of several second messenger systems. The results indicate that excitation–secretion coupling in chromaffin cells, as in fast synapses, is dynamic, with distinct responses to patterned activity that cannot be extrapolated from responses to single stimuli well separated in time.

REFERENCES

Ämmälä C, Eliasson L, Bokvist K, Larsson O, Ashcroft FM, Rorsman P (1993) Exocytosis elicited by action potentials and voltage-clamp calcium currents in individual mouse pancreatic B-cells. J Physiol (Lond) 472:665–688.

Ämmälä C, Eliasson L, Bokvist K, Berggren P-O, Honkanen RE, Sjőholm Å, Rorsman P (1994) Activation of protein kinases and inhibition of protein phosphatases play a central role in the regulation of exocytosis in mouse pancreatic β cells. Proc Natl Acad Sci USA 91:4343–4347.

Artalejo CR, Mogul DJ, Perlman RL, Fox AP (1991) Three types of bovine chromaffin cell Ca^{2+} channels: facilitation increases the opening probability of a 27 pS channel. J Physiol (Lond) 444:213–240.

Artalejo CR, Adams ME, Fox AP (1994) Three types of Ca^{2+} channel trigger secretion with different efficacies in chromaffin cells. Nature 367:72–76.

Augustine GJ, Neher E (1992) Calcium requirements for secretion in bovine chromaffin cells. J Physiol (Lond) 450:247–271.

Bruns D, Jahn R (1995) Real-time measurement of transmitter release from single synaptic vesicles. Nature 377:62–65.

Burgoyne RD (1991) Control of exocytosis in adrenal chromaffin cells. Biochem Biophys Acta 1071:174–202.

Burgoyne RD (1995) Fast exocytosis and endocytosis triggered by depolarisation in single adrenal chromaffin cells before rapid Ca^{2+} current run-down. Pflügers Arch 430:213–219.

Chow RH, Klingauf J, Heinemann C, Zucker RS, Neher E (1996) Mechanisms determining the time course of secretion in neuroendocrine cells. Neuron 16:369–376.

Engisch KL, Nowycky MC (1996) Calcium dependence of large dense-cored vesicle exocytosis evoked by calcium influx in bovine adrenal chromaffin cells. J Neurosci 16:1359–1369.

Engisch KL, Nowycky MC (1997) Compensatory and excess retrieval: two types of endocytosis following single step depolarizations in bovine chromaffin cells. J Physiol, in press.

Fidler N, Fernandez JM (1989) Phase tracking: an improved phase detection technique for cell membrane capacitance measurements. Biophys J 56:1153–1162.

Fisher SA, Fischer TM, Carew TJ (1997) Multiple overlapping processes underlying short-term synaptic enhancement. Trends Neurosci 20:170–177.

Fomina AF, Levitan ES (1995) Three phases of TRH-induced facilitation of exocytosis by single lactotrophs. J Neurosci 15:4982–4991.

Gillis KD, Mossner R, Neher E (1996) Protein kinase C enhances exocytosis from chromaffin cells by increasing the size of the readily releasable pool of secretory granules. Neuron 16:1209–1220.

Giovannucci DR, Stuenkel EL (1997) Regulation of secretory granule recruitment and exocytosis at rat neurohypophysial nerve endings. J Physiol (Lond) 498:735–751.

Hehl S, Golard A, Hille B (1996) Involvement of mitochondria in intracellular calcium sequestration by rat gonadotropes. Cell Calcium 20:515–524.

Heidlelberger R, Heinemann C, Neher E, Matthews G (1994) Calcium dependence of rate of exocytosis in a synaptic terminal. Nature 371:513–515.

Heinemann C, von Rüden L, Chow RH, Neher E (1993) A two-step model of secretion control in neuroendocrine cells. Pflügers Arch 424:105–112.

Heinemann C, Chow RH, Neher E, Zucker RS (1994) Kinetics of the secretory response in bovine chromaffin cells following flash photolysis of caged Ca^{2+}. Biophys J 67:2456–2557.

Horn R, Marty A (1988) Muscarinic activation of ionic currents measured by a new whole-cell recording method. J Gen Physiol 92:145–159.

Horrigan FT, Bookman RJ (1994) Releasable pools and the kinetics of exocytosis in adrenal chromaffin cells. Neuron 13:1119–1129.

Hsu S-F, Jackson MB (1996) Rapid exocytosis and endocytosis in nerve terminals of the rat posterior pituitary. J Physiol (Lond) 494:539–553.

Huang L-YM, Neher E (1996) Ca^{2+}-dependent exocytosis in the somata of dorsal root ganglion neurons. Neuron 17:135–145.

Joshi C, Fernandez JM (1988) Capacitance measurements. An analysis of the phase detector technique used to study exocytosis and endocytosis. Biophys J 53:885–892.

Katz B, Miledi R (1968) The role of calcium in neuromuscular facilitation. J Physiol (Lond) 195:481–493.

Kawagoe KT, Zimmerman JB, Wightman RN (1993) Principles of voltammetry and microelectrode surface states. J Neurosci Methods 48:225–240.

Klingauf J, Neher E (1997) Modeling buffered Ca^{2+} diffusion near the membrane: implications for secretion in neuroendocrine cells. Biophys J 72:674–690.

Lim NF, Nowycky MC, Bookman RJ (1990) Direct measurement of exocytosis and calcium currents in single vertebrate nerve terminals. Nature 344:449–451.

Magleby KL (1987) Short-term changes in synaptic efficacy. In: Synaptic function (Edelman GM, Gall WE, Cowan WM, eds), pp 21–56. New York: Wiley.

Mollard P, Seward EP, Nowycky MC (1995) Activation of nicotinic receptors triggers exocytosis from bovine chromaffin cells in the absence of membrane depolarization. Proc Natl Acad Sci USA 92:3065–3069.

Neher E, Marty A (1982) Discrete changes of cell membrane capacitance observed under conditions of enhanced secretion in bovine adrenal chromaffin cells. Proc Natl Acad Sci USA 79:6712–6716.

Neher E, Zucker RS (1993) Multiple calcium-dependent processes related to secretion in bovine chromaffin cells. Neuron 10:21–30.

Nowycky MC, Pinter MJ (1993) Time course of calcium and calcium-bound buffer transients in a model cell. Biophys J 64:77–91.

Peng Y-Y, Zucker RS (1993) Release of LHRH is linearly related to the time integral of presynaptic Ca^{2+} elevation above a threshold level in bullfrog sympathetic ganglia. Neuron 10:465–473.

Rorsman P, Ämmälä C, Berggren P-O, Bokvist K, Larsson O (1992) Cytoplasmic calcium transients due to single action potentials and voltage-clamp depolarizations in mouse pancreatic B-cells. EMBO J 11:2877–2884.

Sala F, Hernandez-Cruz A (1990) Calcium diffusion modeling in a

spherical neuron. Relevance of buffering properties. Biophys J 57:313–324.

Sejnowski TJ (1996) Synapses get smarter. Nature 382:759–760.

Seward EP, Nowycky MC (1996) Kinetics of stimulus-coupled secretion in dialyzed bovine chromaffin cells in response to trains of depolarizing pulses. J Neurosci 16:553–562.

Seward EP, Chernevskaya NI, Nowycky MC (1995) Exocytosis in peptidergic nerve terminals exhibits two calcium sensitive phases during pulsatile calcium entry. J Neurosci 15:3390–3399.

Stuenkel EL (1994) Regulation of intracellular calcium and calcium buffering properties of rat isolated neurohypophysial nerve endings. J Physiol (Lond) 481:251–271.

Thomas P, Surprenant A, Almers W (1990) Cytosolic Ca^{2+}, exocytosis, and endocytosis in single melanotrophs of the rat pituitary. Neuron 5:723–733.

Thomas P, Wong JG, Lee AK, Almers W (1993) A low affinity Ca^{2+} receptor controls the final steps in peptide secretion from pituitary melanotrophs. Neuron 11:93–104.

Verhage M, McMahon HT, Ghijsen WEJM, Boomsma F, Scholten G, Wiegant VM, Nicholls DG (1991) Differential release of amino acids, neuropeptides, and catecholamines from isolated nerve terminals. Neuron 6:517–524.

Vitale ML, Rodriguez del Castillo A, Tchakarov L, Trifaro J-M (1991) Cortical filamentous actin disassembly and scinderin redistribution during chromaffin cell stimulation precede exocytosis, a phenomenon not exhibited by gelsolin. J Cell Biol 113:1057–1067.

Vitale ML, Seward EP, Trifaro J-M (1995) Chromaffin cell cortical actin network dynamics control the size of the release-ready vesicle pool and the initial rate of exocytosis. Neuron 14:353–363.

von Rüden L, Neher E (1993) A Ca-dependent early step in the release of catecholamines from adrenal chromaffin cells. Science 262:1061–1065.

Wightman RM, Jankowski JA, Kennedy RT, Kawagoe KT, Schroeder TJ, Leszczyszyn DJ, Near JA, Diliberto Jr EJ, Viveros OH (1991) Temporally resolved catecholamine spikes correspond to single vesicle release from individual chromaffin cells. Proc Natl Acad Sci USA 88:10754–10758.

Yamada WM, Zucker RS (1992) Time course of transmitter release calculated from simulations of a calcium diffusion model. Biophys J 61:671–682.

Zador AM, Dobrunz LE (1997) Dynamic synapses in the cortex. Neuron 19:1–4.

Zucker RS (1996) Exocytosis: a molecular and physiological perspective. Neuron 17:1049–1055.